Two-loop $\mathcal{N} = 2$ SQCD amplitudes with external matter from iterated cuts

Gregor Kälin,[a] **Gustav Mogull,**[a] **and Alexander Ochirov**[b]

[a]*Department of Physics and Astronomy, Uppsala University, 75108 Uppsala, Sweden*
[b]*ETH Zürich, Institut für Theoretische Physik, Wolfgang-Pauli-Str. 27, 8093 Zürich, Switzerland*
E-mail: gregor.kaelin@physics.uu.se,
gustav.mogull@physics.uu.se, aochirov@phys.ethz.ch

ABSTRACT: We develop an iterative method for constructing four-dimensional generalized unitarity cuts in $\mathcal{N} = 2$ supersymmetric Yang-Mills (SYM) theory coupled to fundamental matter hypermultiplets ($\mathcal{N} = 2$ SQCD). For iterated two-particle cuts, specifically those involving only four-point amplitudes, this implies simple diagrammatic rules for assembling the cuts to any loop order, reminiscent of the rung rule in $\mathcal{N} = 4$ SYM. By identifying physical poles, the construction simplifies the task of extracting complete integrands. In combination with the duality between color and kinematics we construct all four-point massless MHV-sector scattering amplitudes up to two loops in $\mathcal{N} = 2$ SQCD, including those with matter on external legs. Our results reveal chiral infrared-finite integrands closely related to those found using loop-level BCFW recursion. The integrands are valid in $D \leq 6$ dimensions with external states in a four-dimensional subspace; the upper bound is dictated by our use of six-dimensional chiral $\mathcal{N} = (1, 0)$ SYM as a means of dimensionally regulating loop integrals.

KEYWORDS: Scattering Amplitudes, Supersymmetric Gauge Theory, Duality in Gauge Field Theories

Contents

1   Introduction

Supersymmetric Yang-Mills (SYM) theories are well known to have simpler scattering amplitudes than the most physically interesting gauge theory — quantum chromodynamics (QCD). In planar $\mathcal{N} = 4$ SYM theory, for instance, modern methods have enabled five-loop six-point amplitude computations [1], with the four- and five-point amplitudes known to all loop orders for more than a decade [2, 3]. Even more is known about amplitude integrands in $\mathcal{N} = 4$ SYM, with all-loop n-point results in the maximally helicity-violating (MHV) sector [4–6], their two-loop extensions beyond MHV [7], and higher-loop but lower-point results beyond the leading-color (planar) limit [8–13].

Such studies of SYM theories, together with impressive developments beyond next-to-leading order [14–37], have helped mature modern on-shell methods [38–45]. Together with other techniques, these methods are widely used in current state-of-the-art QCD calculations — nowadays involving two-loop five-parton amplitudes [46–53]. Moreover, amplitudes in supersymmetric gauge theories can often be viewed as specific contributions to QCD amplitudes, at least at tree [54–56] and one-loop level [38, 57, 58]. In these ways SYM calculations have paved the way to new results in QCD.

Recent all-loop BCFW constructions of four-dimensional amplitude integrands in $\mathcal{N} = 4$ SYM [4–6] were preceded by a more pedestrian way of constructing integrands, often referred to as the "rung rule" [59, 60]. It is based on an analysis of two- and three-particle unitarity cuts and their iterative structure. The idea is to directly obtain $(L+1)$- from L-loop integrands by attaching rungs to the individual diagrams:

$$\cdots\overset{\overset{\ell_1}{\rightarrow}}{\underset{\underset{\ell_2}{\rightarrow}}{\rule{1cm}{0pt}}}\cdots \;\to\; -i(\ell_1 + \ell_2)^2 \times \cdots\overset{\overset{\ell_1}{\rightarrow}}{\underset{\underset{\ell_2}{\rightarrow}}{\rule{1cm}{0pt}}}\cdots \tag{1.1}$$

where each rung comes with a kinematic factor. Despite its known shortcomings (it does not give unique representations of the integrand, and if one desires integrands obeying color-kinematics duality [61–63] then the results are not always compatible) the rung rule has been instrumental to initial progress in $\mathcal{N} = 4$ SYM.

In this paper we develop an iterative approach for computing generalized unitarity cuts in $\mathcal{N} = 2$ supersymmetric QCD (SQCD),[1] which is reminiscent of the rung rule and helps us construct amplitude integrands. This theory is equivalent to $\mathcal{N} = 2$ SYM coupled to N_f copies of massless $\mathcal{N} = 2$ matter multiplets in the (anti-)fundamental representation of the (arbitrary) gauge group G. It is therefore more similar to ordinary QCD than $\mathcal{N} = 4$ SYM, while retaining considerable simplifications with respect to the former. This makes it an ideal theory from which to study the effect of reducing supersymmetry on the analytic structure of gauge

---

[1]Our methods are in particular inspired by supersum technologies developed in ref. [9].

theories — an open question that is crucial should one wish to extend the impressive progress in $\mathcal{N} = 4$ SYM to QCD.

Our concrete results, obtained using the rung-rule-like iterative structure of the unitarity cuts, are the complete set of massless four-point MHV amplitude integrands up to two loops, including those with external matter states. The one-loop amplitude with four external matter states has already been computed using an orbifold construction [64], the one- and two-loop amplitudes with four external gluons were determined in refs. [65, 66], and the rest were previously unknown. All of these full-color amplitudes are obtained in a form that respects color-kinematics duality [61–63]. They can therefore be used to produce amplitudes in $\mathcal{N} \geq 2$ pure or matter-coupled supergravities via an array of related double-copy constructions [61, 62, 64, 65, 67–75]. Other four-point one- and two-loop results in $\mathcal{N} = 2$ SQCD include refs. [76–79].

An intriguing new aspect of our approach is the appearance of Dirac traces in the kinematic numerators, which make infrared (IR) properties manifest. Their structure echoes the BCFW-derived expressions in $\mathcal{N} = 4$ SYM, which are known for having well-behaved IR structure; they are also similar to traces appearing in the planar two-loop all-plus amplitudes in non-supersymmetric Yang-Mills theory [80], which are well known thanks to their one-loop-like simplicity [46–48, 81–84].[2] A careful exposition of the IR properties of the two-loop $\mathcal{N} = 2$ SQCD integrands will be reported elsewhere, while in this paper we limit ourselves to explanatory comments during the derivation of our results.

The paper is organized as follows. In section 2 we review the relevant aspects of $\mathcal{N} = 2$ SQCD and its scattering amplitudes, and introduce the necessary tools to deal with color-kinematics duality in this theory. In section 3 we compare the structure of iterated two-particle cuts in this theory with that in $\mathcal{N} = 4$ SYM, and formulate diagrammatic generalized rung rules for the former. We use these rules in sections 4 and 5 to motivate — and, in some cases, fully derive — the kinematic numerators of all four-point amplitudes in $\mathcal{N} = 2$ SQCD, first at one loop and then at two loops. In section 6 we show the limits of applicability of our rung rules by studying more general unitarity cuts. We conclude in section 7 by discussing the interesting features of our results and their derivations, and outline our next steps in the analysis of the integrand structure of (S)QCD.

2 Review: $\mathcal{N} = 2$ SQCD

In this section we explain our approach to scattering amplitudes in $\mathcal{N} = 2$ SQCD, to a considerable degree following refs. [65, 66] but updating the notation as necessary to prepare for later sections. In particular, we introduce a new notation to compactly

---

[2]In fact, local-integrand representations of all-plus amplitudes were inspired by those of $\mathcal{N} = 4$ SYM amplitudes based on a dimension-shifting relationship between their one-loop integrands [85] which persists at two loops.

write four-point tree-level amplitudes involving fundamental hypermultiplets on external legs. We also summarize the off-shell constraints to be placed on kinematic numerators, in addition to those required by color-kinematics duality [61, 62].

2.1 On-shell particle content

The on-shell content of four-dimensional $\mathcal{N} = 2$ SQCD is most easily described by comparison with that of $\mathcal{N} = 4$ SYM. The latter contains $2^4 = 16$ states, and forms a vector supermultiplet [86]:

$$\mathcal{V}_{\mathcal{N}=4}(\eta^I) = A^+ + \eta^I \psi_I^+ + \frac{1}{2}\eta^I \eta^J \varphi_{IJ} + \frac{1}{3!}\epsilon_{IJKL}\eta^I \eta^J \eta^K \psi_-^L + \eta^1 \eta^2 \eta^3 \eta^4 A_- \, . \quad (2.1)$$

The four-dimensional chiral superspace coordinates η^I carry SU(4) R-symmetry indices $\{I, J, \ldots\}$. For later use, let us remark that this multiplet is CPT self conjugate and can equally well be written in terms of anti-chiral superspace coordinates $\bar{\eta}_I$ using

$$\mathcal{V}_{\mathcal{N}=4}(\bar{\eta}_I) = \int d^4\eta \, e^{\eta^I \bar{\eta}_I} \mathcal{V}_{\mathcal{N}=4}(\eta^I) = A_- + \bar{\eta}_I \psi_-^I + \cdots + \bar{\eta}_1 \bar{\eta}_2 \bar{\eta}_3 \bar{\eta}_4 A^+ \, , \quad (2.2)$$

where the measure is $d^4\eta = d\eta^1 d\eta^2 d\eta^3 d\eta^4$.

The $\mathcal{N} = 4$ multiplet naturally decomposes on η^3 and η^4 into $\mathcal{N} = 2$ multiplets:

$$\mathcal{V}_{\mathcal{N}=4} = V_{\mathcal{N}=2}^+ + \eta^3 \Phi_{\mathcal{N}=2} + \eta^4 \overline{\Phi}_{\mathcal{N}=2} + \eta^3 \eta^4 V_{\mathcal{N}=2}^- \, . \quad (2.3)$$

Here the $\mathcal{N} = 2$ vector multiplets are

$$V_{\mathcal{N}=2}^+(\eta^I) = A^+ + \eta^I \psi_I^+ + \eta^1 \eta^2 \varphi_{12} \, , \qquad V_{\mathcal{N}=2}^-(\eta^I) = \varphi_{34} + \epsilon_{I34J}\eta^I \psi_-^J + \eta^1 \eta^2 A_- \, , \quad (2.4)$$

where the SU(2) indices $I, J = 1, 2$ are inherited from SU(4); the hypermultiplets (hypers) are

$$\Phi_{\mathcal{N}=2}(\eta^I) = \psi_3^+ - \eta^I \varphi_{I3} + \eta^1 \eta^2 \psi_-^4 \, , \qquad \overline{\Phi}_{\mathcal{N}=2}(\eta^I) = \psi_4^+ - \eta^I \varphi_{I4} - \eta^1 \eta^2 \psi_-^3 \, . \quad (2.5)$$

All four have $\mathcal{N} = 2$ supersymmetries represented by the remaining Grassmann variables η^1 and η^2. Moreover, $V_{\mathcal{N}=2}^+$ is related to $V_{\mathcal{N}=2}^-$ by CPT conjugation, and likewise for $\Phi_{\mathcal{N}=2}$ and $\overline{\Phi}_{\mathcal{N}=2}$.

The on-shell content of $\mathcal{N} = 2$ SQCD is obtained by switching the representation of the hypers $\Phi_{\mathcal{N}=2}$ and $\overline{\Phi}_{\mathcal{N}=2}$ from the adjoint to the fundamental and anti-fundamental representations, respectively. This explicitly breaks supersymmetry on η^3 and η^4, but not on η^1 and η^2. Furthermore, the hypers can be generalized to an arbitrary number $N_f = \delta_\alpha^\alpha$ of flavors by attaching flavor indices $\{\alpha, \beta, \ldots\}$ to them, as in $(\Phi_{\mathcal{N}=2})^\alpha$ and $(\overline{\Phi}_{\mathcal{N}=2})_\alpha$. Alternatively, the flavor indices can be conflated with the color indices, implying reducible gauge-group representations for the matter multiplets. In this paper will use the tree amplitudes for $N_f = 1$ to construct

hel. \ th.	$\mathcal{N}=4$ SYM	$\mathcal{N}=2$ SQCD				QCD		
				$\overbrace{\qquad}^{N_f}$			$\overbrace{\qquad}^{N_f}$	
$+1$	1	1				1		
$+1/2$	4	2		1	1		1	1
0	6	1	1	2	2			
$-1/2$	4		2	1	1		1	1
-1	1	1				1		
rep.	adj.	adj.		$\dfrac{\text{fund.}}{\overline{\text{fund.}}}$		adj.	$\dfrac{\text{fund.}}{\overline{\text{fund.}}}$	

Table 1: Helicity content of $\mathcal{N}=2$ supersymmetric QCD in comparison to $\mathcal{N}=4$ super-Yang-Mills theory and conventional QCD. For these theories, the helicities and the representations of the particles are listed in the left column and the lower row, respectively.

unitarity cuts; the diagrammatic form of the resulting loop integrands will allow for an arbitrary N_f.

By analogy to QCD, $V_{\mathcal{N}=2}^{+}$ and $V_{\mathcal{N}=2}^{-}$ act as positive- and negative-helicity gluons, A^{+} and A_{-}, and can be regarded as their respective on-shell supersymmetrizations. The hypermultiplets $(\Phi_{\mathcal{N}=2})^{\alpha}$ and $(\overline{\Phi}_{\mathcal{N}=2})_{\alpha}$ play the roles of massless quarks and anti-quarks. In this way, $\mathcal{N}=2$ SQCD can be viewed as the middle ground between $\mathcal{N}=4$ SYM and the actual QCD, as illustrated in table 1. Although it is less well studied than the other two, its one-loop MHV and NMHV amplitudes are known for any number of external gluons [39, 87, 88] via their relation to those in $\mathcal{N}=1,2,4$ SYM [38].

2.2 Tree-level amplitudes

Tree-level $\mathcal{N}=2$ SQCD amplitudes are simply related to those of $\mathcal{N}=4$ SYM. In the maximally helicity-violating (MHV) sector, to which we specialize in this paper, planar tree-level $\mathcal{N}=4$ SYM amplitudes are given by the famous Parke-Taylor formula [86, 89]:[3]

$$A_n^{(0),\text{MHV}}\big(\mathcal{V}_{\mathcal{N}=4}, \mathcal{V}_{\mathcal{N}=4}, \ldots, \mathcal{V}_{\mathcal{N}=4}\big) = \frac{i\delta^8(Q)}{\langle 12\rangle\langle 23\rangle\cdots\langle n1\rangle}\,. \qquad (2.6)$$

Here the Grassmann delta function imposes conservation of supercharges; for $\mathcal{N}$ supersymmetries it is

$$\delta^{2\mathcal{N}}(Q) = \delta^{2\mathcal{N}}\bigg(\sum_{i=1}^{n} |i\rangle\eta_i\bigg) = \prod_{I=1}^{\mathcal{N}}\sum_{i<j}^{n}\eta_i^I\langle i\,j\rangle\eta_j^I\,. \qquad (2.7)$$

Tree-level $\mathcal{N}=2$ SQCD amplitudes with $N_f=1$ massless hypermultiplet flavors are obtained by projecting out the relevant multiplets using the decomposition given

---

[3]We adopt the usual spinor-helicity notation — see for example refs. [54, 90].

in eq. (2.3). The two extra superspace coordinates η^3 and η^4, associated with the two broken supersymmetries, serve to identify the multiplets: $\Phi_{\mathcal{N}=2}$ carries η^3, $\overline{\Phi}_{\mathcal{N}=2}$ carries η^4, $V_{\mathcal{N}=2}^+$ carries neither, and $V_{\mathcal{N}=2}^-$ carries both. Several n-point examples are given in ref. [66].

In this paper we will mostly use four-point amplitudes. In order to track the $\mathcal{N}=2$ multiplets on their external legs, we introduce the superspace combination

$$\kappa_{(ab)(cd)}(1,2,3,4) \equiv \frac{[12][34]}{\langle 12\rangle\langle 34\rangle}\delta^4(Q)\eta_a^3\langle a\,b\rangle\eta_b^3\eta_c^4\langle c\,d\rangle\eta_d^4\,, \tag{2.8}$$

where $\{a,b,c,d\} \in \{1,2,3,4\}$. Here the spinor-helicity prefactor is permutation invariant and is familiar from the commonly used $\mathcal{N}=4$ amplitude prefactor

$$\kappa(1,2,3,4) \equiv \frac{[12][34]}{\langle 12\rangle\langle 34\rangle}\delta^8(Q)\,. \tag{2.9}$$

In refs. [65, 66] a similar notation was used to label the two anti-chiral $V_{\mathcal{N}=2}^-$ vector multiplets in the MHV sector: $\kappa_{ab} \equiv \kappa_{(ab)(ab)}$. Our updated notation is more flexible, as it allows us to also track the hypermultiplets $\Phi_{\mathcal{N}=2}$ and $\overline{\Phi}_{\mathcal{N}=2}$ on external legs. For instance, we can now compactly write

$$A_4^{(0),\text{MHV}}(V_{\mathcal{N}=2}^-, V_{\mathcal{N}=2}^+, V_{\mathcal{N}=2}^-, V_{\mathcal{N}=2}^+) = -\frac{i}{st}\kappa_{(13)(13)} = -\frac{i}{st}\kappa_{13}\,, \tag{2.10a}$$

$$A_4^{(0),\text{MHV}}(V_{\mathcal{N}=2}^-, \Phi_{\mathcal{N}=2}, \overline{\Phi}_{\mathcal{N}=2}, V_{\mathcal{N}=2}^+) = -\frac{i}{st}\kappa_{(12)(13)}\,, \tag{2.10b}$$

$$A_4^{(0),\text{MHV}}(\Phi_{\mathcal{N}=2}, \overline{\Phi}_{\mathcal{N}=2}, \Phi_{\mathcal{N}=2}, \overline{\Phi}_{\mathcal{N}=2}) = -\frac{i}{st}\kappa_{(13)(24)}\,, \tag{2.10c}$$

$$A_4^{(0),\text{MHV}}(\Phi_{\mathcal{N}=2}, \Phi_{\mathcal{N}=2}, \overline{\Phi}_{\mathcal{N}=2}, \overline{\Phi}_{\mathcal{N}=2}) = -\frac{i}{st}\kappa_{(12)(34)}\,, \tag{2.10d}$$

where $s = (p_1+p_2)^2$ and $t = (p_2+p_3)^2$ are the usual Mandelstam variables.

Using CPT invariance of the theory we can equally well study $\overline{\text{MHV}}$ amplitudes. These are related to the MHV by exchanging $|i\rangle \leftrightarrow |i]$ and $\eta_i^I \leftrightarrow \bar{\eta}_{i,I}$. For instance, the n-point tree-level $\overline{\text{MHV}}$ amplitude is also given by a Parke-Taylor formula:

$$A_n^{(0),\overline{\text{MHV}}}(\mathcal{V}_{\mathcal{N}=4}, \mathcal{V}_{\mathcal{N}=4}, \ldots, \mathcal{V}_{\mathcal{N}=4}) = \frac{i\delta^8(\bar{Q})}{[12][23]\cdots[n1]}\,, \tag{2.11}$$

where the anti-chiral supermomentum-conserving delta function is defined as

$$\delta^{2\mathcal{N}}(\bar{Q}) = \prod_{I=1}^{\mathcal{N}}\sum_{i<j}^n \bar{\eta}_i^I[i\,j]\bar{\eta}_j^I\,. \tag{2.12}$$

To compare amplitudes formulated in different superspaces we switch between chiral and anti-chiral superspace coordinates using Fourier transforms:

$$A_n(\eta_i^I) = \int \mathrm{d}^4\bar{\eta}_1\cdots \mathrm{d}^4\bar{\eta}_n e^{\bar{\eta}_{1,I}\eta_1^I}\cdots e^{\bar{\eta}_{n,I}\eta_n^I}A_n(\bar{\eta}_{i,I})\,. \tag{2.13}$$

Note that even with $\mathcal{N} = 2$ supersymmetries we continue to use the four-dimensional Grassmann integration $\mathrm{d}^4\eta_i$ — the superspace variables of the broken supersymmetry are retained in order to discern between the $\mathcal{N} = 2$ multiplets.

At four points the MHV and $\overline{\text{MHV}}$ amplitudes are equivalent, so related by the Fourier transform (2.13). We can therefore also track the external state configuration using

$$\bar{\kappa}_{(ab)(cd)}(1,2,3,4) \equiv \frac{\langle 12 \rangle \langle 34 \rangle}{[12][34]} \delta^4(\bar{Q}) \bar{\eta}_{a,3}[a\,b] \bar{\eta}_{b,3} \bar{\eta}_{c,4}[c\,d] \bar{\eta}_{d,4} \,. \tag{2.14}$$

Under the Fourier transform (2.13) this maps into $\kappa_{(\overline{ab})(\overline{cd})}(1,2,3,4)$, where a barred pair of indices $\{\overline{a,b}\} \equiv \{1,2,3,4\} \setminus \{a,b\}$ denotes the complement with respect to the set of external labels.

2.3 Loop-level amplitudes

Proceeding now to consider loop-level amplitudes, we adopt diagrammatic representations from the outset. In a general Yang-Mills theory, the trivalent nature of the gauge group generators allows us to write any L-loop amplitude as a sum of cubic graphs:

$$\mathcal{A}_n^{(L)} = i^{L-1} g^{n+2L-2} \sum_{\text{cubic graphs } \Gamma_i} \int \frac{\mathrm{d}^{LD}\ell}{(2\pi)^{LD}} \frac{1}{S_i} \frac{n_i c_i}{D_i} \,. \tag{2.15}$$

Here g is the coupling, S_i are the symmetry factors, D_i are the usual products of massless propagators, and n_i are the kinematic numerators associated with each graph, depending on both external and loop momenta. To regulate potentially divergent integrals, we use dimensional regularization in $D = 4 - 2\epsilon$ dimensions. Finally, we assume $N_f = 1$ hypermultiplet flavors; one can generalize to $N_f \neq 1$ by assigning flavor-conserving delta functions to each diagram, with $N_f = \delta_\alpha^\alpha$ for closed matter loops (see refs. [55, 56, 63] for more details).

One of the main advantages of such a cubic representation is that the color factors c_i are unambiguously assigned to the graphs. There are two kinds of trivalent vertices: pure-adjoint, and those with a particle in each of the adjoint, fundamental and anti-fundamental representations. These are associated with the structure constant $\tilde{f}^{abc} = \text{tr}([T^a, T^b]T^c)$ and generator $T_{i\bar{j}}^a$, respectively:[4]

$$\tilde{f}^{abc} = c\left(a \rightsquigarrow \begin{matrix} b \\ c \end{matrix}\right), \qquad T_{i\bar{j}}^a = c\left(i \blacktriangleleft \begin{matrix} a \\ \bar{j} \end{matrix}\right). \tag{2.16}$$

Both are antisymmetric: $\tilde{f}^{abc} = -\tilde{f}^{acb}$, $T_{i\bar{j}}^a \equiv -T_{\bar{j}i}^a$ (the latter relationship defines $T_{\bar{i}j}^a$). Fundamental structure constants are normalized such that $\text{tr}(T^a T^b) = \delta^{ab}$.

We seek loop-level amplitude representations obeying color-kinematics duality [61, 62]. In this case, the same linear identities satisfied by the color factors

---

[4]In this paper, we label cubic diagrams by their graphical representations. Their explicit layout encodes a sign due to the antisymmetry of the vertices.

c_i should also be satisfied by the kinematic numerators n_i, which we refer to as color-dual. Such relationships include commutation relations

$$\tilde{f}^{ba_3a_4}T^b_{i_1\bar{i}_2} = T^{a_3}_{i_1\bar{j}}T^{a_4}_{\bar{j}\bar{i}_2} - T^{a_4}_{i_1\bar{j}}T^{a_3}_{\bar{j}\bar{i}_2} = [T^{a_3}, T^{a_4}]_{i_1\bar{i}_2}\,,$$

$$c\left(\begin{array}{c}\text{4}\\\text{3}\end{array}\!\!\!\!\!\!\!\!\!\!\!\!\!\!\!\!\!\!\raisebox{0pt}{\includegraphics{diag}}\!\!\!\!\!\!\!\!\begin{array}{c}\text{1}\\\text{2}\end{array}\right) = c\left(\begin{array}{c}\text{4}\\\text{3}\end{array}\!\!\!\!\raisebox{0pt}{}\!\!\!\!\begin{array}{c}\text{1}\\\text{2}\end{array}\right) - c\left(\begin{array}{c}\text{3}\\\text{4}\end{array}\!\!\!\!\raisebox{0pt}{}\!\!\!\!\begin{array}{c}\text{1}\\\text{2}\end{array}\right)\,,$$
(2.17)

and their adjoint-representation counterparts — the Jacobi identities

$$\tilde{f}^{a_1a_2b}\tilde{f}^{ba_3a_4} = \tilde{f}^{a_4a_1b}\tilde{f}^{ba_2a_3} - \tilde{f}^{a_2a_4b}\tilde{f}^{ba_3a_1}\,,$$

$$c\left(\begin{array}{c}\text{4}\\\text{3}\end{array}\!\!\!\!\raisebox{0pt}{}\!\!\!\!\begin{array}{c}\text{1}\\\text{2}\end{array}\right) = c\left(\begin{array}{c}\text{4}\\\text{3}\end{array}\!\!\!\!\raisebox{0pt}{}\!\!\!\!\begin{array}{c}\text{1}\\\text{2}\end{array}\right) - c\left(\begin{array}{c}\text{3}\\\text{4}\end{array}\!\!\!\!\raisebox{0pt}{}\!\!\!\!\begin{array}{c}\text{1}\\\text{2}\end{array}\right)\,.$$
(2.18)

Color-kinematics duality requires that

$$c_i = c_j - c_k \qquad \Leftrightarrow \qquad n_i = n_j - n_k\,,$$
(2.19)

The usual motivation for finding so-called color-dual representations is to enable use of the double copy [61, 62], which allows supergravity amplitudes to be obtained by replacing the color factors c_i with a second copy of the kinematic numerators n_i in the amplitude (2.15). Fundamental-representation hypers play an important role when dealing with $\mathcal{N} < 4$ supergravities, for example as they allow unwanted additional vector multiplets to be subtracted from the resulting supergravity multiplet [65]. For instance, refs. [65, 66] described how pure $\mathcal{N} = 4$ supergravity amplitudes could be obtained from a double copy of $\mathcal{N} = 2$ SYM with itself, the hypermultiplets being used internally to remove unwanted $\mathcal{N} = 4$ SYM multiplets from the supergravity theory.

There are, however, considerable advantages to finding color-dual representations even if the goal is merely efficient computation of gauge-theory amplitudes. First, such representations are cubic, so the assignment of color factors to diagrams is trivial (for alternative non-cubic constructions of full-color integrands from unitarity cuts see e.g. refs. [47, 91, 92]). Moreover, the kinematic numerators being interlinked by commutation and Jacobi relations implies that only a limited subset of the numerators need to be calculated directly. The corresponding graphs, which are referred to as masters, are chosen to ensure that the numerators of all other graphs can be obtained using commutation and Jacobi identities. For instance, using the commutation relation (2.17) implies

$$n\left(\begin{array}{c}\text{4}\\\text{3}\end{array}\!\!\!\!\raisebox{0pt}{}\!\!\!\!\begin{array}{c}\text{1}\\\text{2}\end{array}\right) = n\left(\begin{array}{c}\text{4}\\\text{3}\end{array}\!\!\!\!\raisebox{0pt}{}\!\!\!\!\begin{array}{c}\text{1}\\\text{2}\end{array}\right) - n\left(\begin{array}{c}\text{4}\\\text{3}\end{array}\!\!\!\!\raisebox{0pt}{}\!\!\!\!\begin{array}{c}\text{2}\\\text{1}\end{array}\right)\,.$$
(2.20)

In this case, the triangle is uniquely determined by the two boxes; these, in turn, are related by a symmetry through the horizontal axis (after relabeling $p_3 \leftrightarrow p_4$). The

box is in this case a master: it is on these masters that we will focus our attention in later sections.

In general, the existence of a consistent set of color-dual numerators is not trivial. At tree level, it is proven [93, 94] for gauge theories, in which color-ordered amplitudes satisfy the BCJ relations [61, 95–97]. For (super-)Yang-Mills theories with arbitrary fundamental matter, which is less studied, the corresponding BCJ relations [63, 65] have been proven in the case of QCD [98].

The task of finding color-dual representations is further complicated by the fact that, for a given amplitude, such representations are generally not unique. For this reason, a large part of ref. [66] was devoted to finding additional constraints to be imposed on the numerators, with the intention of shrinking the space of allowed solutions while manifesting certain desirable properties. These constraints also reduce the number of masters to be computed. In the remainder of this section we discuss the constraints that we have found helpful. Note that not all the integrands presented here have all the properties presented below; appendix B summarizes the various representations and their properties.

2.3.1 Two-term identities

If imposed, the two-term identities require that, for indistinguishable matter multiplets,

$$c\left(\begin{array}{c} 4 \\ 3 \end{array} \!\!\!\!\!\!\!\!\!\! \begin{array}{c} 1 \\ 2 \end{array} \right) \stackrel{?}{=} c\left(\begin{array}{c} 4 \\ 3 \end{array} \!\!\!\!\!\!\!\!\!\! \begin{array}{c} 1 \\ 2 \end{array} \right). \tag{2.21}$$

Although this is not true in general, it holds if the gauge group is chosen as $G = \mathrm{U}(1)$, or for specific tensor representations of $\mathrm{U}(N_c)$ [65]. Like the commutation and Jacobi relations, we impose these identities on the numerators whose graphs contain internal subgraphs of the above form. For instance, these one-loop box and triangle numerators are equated:

$$n\left(\begin{array}{c} 4 \\ 3 \end{array} \!\!\!\!\!\!\!\!\!\! \begin{array}{c} 1 \\ 2 \end{array} \right) = n\left(\begin{array}{c} 4 \\ 3 \end{array} \!\!\!\!\!\!\!\!\!\! \begin{array}{c} 1 \\ 2 \end{array} \right). \tag{2.22}$$

One can also regard the two-term identities as their own kind of commutation relations, the difference being that the u-channel graphs are excluded as their routing of fundamental matter lines is not sensible.

As we shall see in section 3.2.1, the two-term identities have their origin in the structure of the $\mathcal{N} = 2$ cuts, and the diagrammatic rules will help to clarify this. In ref. [66], these identities allowed all numerators with two matter loops to be reduced to those with one matter loop. The two-term identities are equally useful in restricting the set of masters when matter is taken on external legs.

2.3.2 CPT conjugation

Amplitudes respect the CPT invariance of the theory, and we can extend this to a manifest off-shell symmetry acting on individual numerators. CPT conjugation acts by transforming $|i\rangle \leftrightarrow |i]$ and $\eta_i^I \leftrightarrow \bar{\eta}_{i,I}$; graphically, this corresponds to flipping the helicity of external vectors and reversing arrow directions on hypermultiplets. The transformation should correspond to a replacement of $\kappa_{(ab)(cd)}$ by its complement and an additional sign flip of parity-odd terms:

$$n_i(1,2,3,4;\ell_1,\ell_2) = \bar{n}_i(1,2,3,4;\ell_1,\ell_2)|_{\kappa_{(ab)(cd)} \to \kappa_{(\overline{ab})(\overline{cd})}, |i\rangle \leftrightarrow |i]}, \qquad (2.23)$$

where $\bar{n}_i$ stands for the numerator of the graph with flipped arrows on matter lines; $\{\overline{a,b}\} \equiv \{1,2,3,4\} \setminus \{a,b\}$. For instance, we could equate

$$n \left(\begin{array}{c} 4 \\ 3 \end{array} \!\!\!\!\! \begin{array}{c} 1 \\ 2 \end{array} \right) = n \left(\begin{array}{c} 4 \\ 3 \end{array} \!\!\!\!\! \begin{array}{c} 1 \\ 2 \end{array} \right) \Bigg|_{\kappa_{(ab)(cd)} \to \kappa_{(\overline{ab})(\overline{cd})}, |i\rangle \leftrightarrow |i]} . \qquad (2.24)$$

Note that a change of direction of external hyper lines together with the conjugation of the indices of κ lands us back on the same external state configuration as we started from.

2.3.3 Matter-reversal symmetry

The matter multiplets $\Phi_{\mathcal{N}=2}$ and $\overline{\Phi}_{\mathcal{N}=2}$ are identical up to R-symmetry indices and the gauge-group representation, which leads to another potential off-shell symmetry of the numerators. In ref. [66] only vector multiplets were allowed on external legs, so the symmetry was invariance under arrow reversal for all numerators containing matter loops. The symmetry held for each matter loop individually.

   With hypermultiplets on external legs the situation is more subtle. One cannot simply equate numerators with reversed hypermultiplets, as they carry different external states. But this is easily remedied: by inspection of the $\mathcal{N}=4$ state decomposition (2.3) the symmetry clearly exchanges $\eta^3 \leftrightarrow \eta^4$ (with no effect on $V_{\mathcal{N}=2}^+$ or $V_{\mathcal{N}=2}^-$). With this additional exchange imposed, we can implement the same identity, for instance

$$n \left(\begin{array}{c} 4 \\ 3 \end{array} \!\!\!\!\! \begin{array}{c} 1 \\ 2 \end{array} \right) = - n \left(\begin{array}{c} 4 \\ 3 \end{array} \!\!\!\!\! \begin{array}{c} 1 \\ 2 \end{array} \right) \Bigg|_{\eta_2^4 \to \eta_2^3, \eta_3^3 \to \eta_3^4} . \qquad (2.25)$$

This symmetry is required if one considers matter multiplets in a pseudo-real representation [71, 99].

2.3.4 Matching with $\mathcal{N}=4$ SYM

As we have already seen in eq. (2.3), the vector multiplet $\mathcal{V}_{\mathcal{N}=4}$'s $2^4 = 16$ states can be distributed between $V_{\mathcal{N}=2}^+$, $V_{\mathcal{N}=2}^-$, $\Phi_{\mathcal{N}=2}$ and $\overline{\Phi}_{\mathcal{N}=2}$. This offers another constraint on the color-dual $\mathcal{N}=2$ SQCD numerators: that summing them over the internal

multiplets corresponding to the on-shell content of $\mathcal{N} = 4$ SYM should reproduce those same numerators. For instance, we can demand that

$$n^{[\mathcal{N}=4]}\left(\vcenter{\hbox{\includegraphics{box1}}}\right) = n\left(\vcenter{\hbox{\includegraphics{box2}}}\right) + n\left(\vcenter{\hbox{\includegraphics{box3}}}\right) + n\left(\vcenter{\hbox{\includegraphics{box4}}}\right) + n\left(\vcenter{\hbox{\includegraphics{box5}}}\right)$$
$$+ n\left(\vcenter{\hbox{\includegraphics{box6}}}\right) + n\left(\vcenter{\hbox{\includegraphics{box7}}}\right) + n\left(\vcenter{\hbox{\includegraphics{box8}}}\right),$$
(2.26)

where in this case a suitable expression for the $\mathcal{N} = 4$ double-box numerator is simply

$$n^{[\mathcal{N}=4]}\left(\vcenter{\hbox{\includegraphics{dbox}}}\right) = s(\kappa_{12} + \kappa_{13} + \kappa_{14} + \kappa_{23} + \kappa_{24} + \kappa_{34}). \qquad (2.27)$$

Here we have projected the $\mathcal{N} = 2$ vector multiplets out of the supersymmetric delta function $\delta^8(Q)$. This statement must be true for kinematic configurations where the propagators are taken on-shell, i.e. on the maximal cut, because summing over these diagrams then simply amounts to taking η^3 and η^4 integrals on the right-hand side. This logic also holds when hypers are taken on external legs. The non-trivial observation is that we can demand it also be true for off-shell loop momenta.

3 Iterated two-particle cuts

In this section we describe the iterative two-particle cut construction, as it applies to both $\mathcal{N} = 4$ and $\mathcal{N} = 2$ SYM in strictly four dimensions (in section 4 we will explain how to find higher-dimensional corrections for the purpose of dimensional regularization). The construction is underpinned by that fact that when two four-point amplitudes are glued together to form a cut, the result is proportional to another four-point tree amplitude. This allows the gluing procedure to be iterated, leading to diagrammatic rules for cut assembly without the need to perform intermediate supersums. As we shall see, in $\mathcal{N} = 4$ SYM this construction leads to the so-called "rung rule" for assembling Mondrian-type diagrams [59, 60, 100].

3.1 $\mathcal{N} = 4$ SYM

To understand the iterated nature of two-particle cuts in $\mathcal{N} = 4$ SYM, we begin with the four-point one-loop s-channel cut

$$\vcenter{\hbox{\includegraphics{cut}}} = \int \mathrm{d}^4\eta_{l_1}\mathrm{d}^4\eta_{l_2} A_4^{(0),\mathrm{MHV}}(1,2,l_1,l_2) A_4^{(0),\mathrm{MHV}}(3,4,-l_2,-l_1)$$
$$= -i\frac{st}{(l_1+p_2)^2(l_1-p_3)^2} A_4^{(0),\mathrm{MHV}}(1,2,3,4). \qquad (3.1)$$

The fact that this cut is proportional to the tree amplitude is a well-known result, following from Green, Schwarz and Brink's original computation of the one-loop amplitude [101]. If we extract the physical poles from the tree amplitudes using the MHV formula

$$A_4^{(0),\text{MHV}}(1,2,3,4) = -\frac{i}{st}\kappa(1,2,3,4)\,, \tag{3.2}$$

then using $s = s_{l_1 l_2}$ (in this case) — where $s_{ij} = (p_i + p_j)^2$, which we extend to include loop momenta — the cut identity can be more compactly written as

$$\int \mathrm{d}^4\eta_{l_1}\mathrm{d}^4\eta_{l_2}\kappa(1,2,l_1,l_2)\kappa(3,4,-l_2,-l_1) = s_{l_1 l_2}^2\kappa(1,2,3,4)\,. \tag{3.3}$$

A similar construction was presented in ref. [9]; for the sake of completeness we give a proof of this relation in appendix A.

3.1.1 $\mathcal{N} = 4$ diagrammatic rules

The two-particle cut being proportional to the tree-level amplitude allows for an iterated construction. We can attach more four-point tree-level amplitudes to the cut and glue two pairs of legs at a time by using eq. (3.3). So any iterated two-particle cut is a product of terms coming from its four-point tree-level amplitudes and two-particle supersums. The following diagrammatic rules summarize the construction:

$$\raisebox{-0.5em}{\includegraphics{}}\; \to\; -\frac{i}{s_{ab}s_{ac}}\,, \qquad \raisebox{-0.5em}{\includegraphics{}}\; \to\; s_{l_1 l_2}^2\,, \qquad \raisebox{-0.5em}{\includegraphics{}}\; \to\; \kappa(q,r,s,t)\,. \tag{3.4}$$

The first rule comes from eq. (3.2); for each tree-amplitude constituent, we must insert its physical poles. The second rule is the result of eq. (3.3); it tells us that a factor $s_{l_1 l_2}^2$ is obtained whenever two tree-level amplitudes are glued together. Finally, the last "external" rule tells us that, once all partons have been assembled, we should multiply by an overall κ factor to encode the configuration of external states.

The s-channel cut from before is now easily assembled:

$$\raisebox{-1em}{\includegraphics{}}\; = \frac{-i}{s_{12}s_{1l_2}} \times s_{l_1 l_2}^2 \times \frac{-i}{s_{34}s_{4(-l_2)}} \times \kappa = -\frac{s_{l_1 l_2}^2 \kappa}{s^2 s_{1l_2} s_{4(-l_2)}}\,. \tag{3.5}$$

The poles are the physical poles of both tree-level constituents. Re-using $s = s_{l_1 l_2}$ to cancel unwanted poles, it becomes clear that the only ones leftover are s_{1l_2} and $s_{4(-l_2)}$. In terms of off-shell numerators,

$$n^{[\mathcal{N}=4]}\left(\raisebox{-1em}{\includegraphics{}}\right) = \kappa \tag{3.6}$$

is the only contributor [101].

3.1.2 The rung rule

The rung rule takes this construction one step further, directly giving off-shell expressions for box-like Mondrian diagrams without the need for cut assembly [59, 100]. In the s-channel cut given above, we noticed a cancellation between kinematic factors $s_{l_1 l_2}$, coming from the gluing rule (3.3), with physical poles coming from the physical tree amplitudes (3.2). The cancellation is completely general, as gluing a four-point tree amplitude to an arbitrary four-point MHV amplitude gives

$$\text{[diagram]} = \frac{-i}{s_{12} s_{1(-l_2)}} \times s_{l_1 l_2}^2 \times \text{[diagram]} = -\frac{i s_{l_1 l_2}}{s_{1(-l_2)}} \times \text{[diagram]} . \qquad (3.7)$$

This suggests that a triangle-like diagram should not contribute as the s_{12} pole is absent. By further cutting into the left tree-level amplitude we obtain an on-shell rung rule:

$$\text{[diagram]} = -i s_{l_1 l_2} \times \text{[diagram]} . \qquad (3.8)$$

In other words, attaching an on-shell rung to an existing cut amounts to multiplication by $-i s_{l_1 l_2}$. The off-shell continuation of this statement for the amplitude numerators is typically written as

$$\text{[diagram]} = -i(\ell_1 + \ell_2)^2 \times \text{[diagram]} , \qquad (3.9)$$

where the legs ℓ_1 and ℓ_2 are now understood to carry unconstrained loop momenta.[5]

For instance, beginning with the box numerator given in eq. (3.6), attaching a first rung gives the two-loop double box numerator [59],

$$n^{[\mathcal{N}=4]}\left(\text{[diagram]} \right) = s \, \kappa . \qquad (3.10)$$

The two possible ways of attaching a second rung give the 3-loop triple-box and "tennis-court" numerators:

$$n^{[\mathcal{N}=4]}\left(\text{[diagram]} \right) = s^2 \, \kappa , \qquad n^{[\mathcal{N}=4]}\left(\text{[diagram]} \right) = s(\ell + p_4)^2 \, \kappa . \qquad (3.11)$$

This pattern agrees with the three-loop amplitude [4, 5, 59].

However, we should recognize the circumstances under which the rung rule is too naïve. While cuts are unique, off-shell numerators are not: we are free to shift terms between numerators by adding terms that vanish on support of the on-shell conditions. So the numerators may require modification, for instance, if

---

[5]In principle, the off-shell continuation of $s_{l_1 l_2}$ to $(\ell_1 + \ell_2)^2$ in eq. (3.9) is not unique. One may, for example, choose $2(\ell_1 \cdot \ell_2)$ instead, thereby ignoring the terms ℓ_1^2 and ℓ_2^2 that vanish on the cut.

- the same diagram contributes to cuts that suggest different on-shell forms;

- additional off-shell constraints — like color duality — are demanded.

A classic example where the rung rule fails to provide color-dual numerators is the 4-point, 3-loop MHV amplitude [62, 102] — the numerators given above are not color-dual. Therefore, as we now proceed to consider $\mathcal{N} = 2$ SQCD, we will use the iteration only to construct cuts, and remember that off-shell numerators may require modification.

3.2 $\mathcal{N} = 2$ SQCD

The iterative cut construction works in $\mathcal{N} = 2$ SYM for the same reason as in $\mathcal{N} = 4$ SYM: because the result of gluing together a pair of tree-level amplitudes is proportional to another tree-level amplitude. The generalization of the supersum (3.3), written in terms of $\kappa_{(ab)(cd)}$ as introduced in section 2.2, is

$$\int \mathrm{d}^4 \eta_{l_1} \mathrm{d}^4 \eta_{l_2} \kappa^{(\mathrm{L})}_{(ab)(cd)} \kappa^{(\mathrm{R})}_{(ef)(gh)} = s_{l_1 l_2} \langle ab \rangle [\overline{cd}] \langle ef \rangle [\overline{gh}] [qr] \langle \overline{st} \rangle \frac{\kappa_{(qr)(st)}}{s_{qr} s_{st}} \,, \qquad (3.12)$$

which we will prove below; we denote

$$\begin{aligned} \kappa^{(\mathrm{L})}_{(ab)(cd)} &= \kappa_{(ab)(cd)}(1, 2, l_1, l_2) \,, & \kappa^{(\mathrm{R})}_{(ef)(gh)} &= \kappa_{(ef)(gh)}(3, 4, -l_2, -l_1) \,, \\ \kappa_{(qr)(st)} &= \kappa_{(qr)(st)}(1, 2, 3, 4) \,, \end{aligned} \qquad (3.13)$$

where $(qr)(st)$ denotes the overall state configuration. Bars denote the complement with respect to external legs on a tree amplitude; for instance, $\{\overline{c, d}\} = \{1, 2, l_1, l_2\} \setminus \{c, d\}$. We omit the overall sign since it depends on the ordering of the complement, which affects the spinor-helicity brackets.

As we shall discuss in section 6, similar relations work for higher-point tree amplitudes. In the conclusions, we will also discuss possible generalizations to $\mathcal{N} = 0$ and $\mathcal{N} = 1$ SYM amplitudes.

3.2.1 $\mathcal{N} = 2$ diagrammatic rules

The relationship (3.12) leads to simple rules for assembling any iterated two-particle cut. For each four-point constituent, regardless of the configuration of external or intermediate states, we include the same physical poles as we did for $\mathcal{N} = 4$ SYM:

$$\begin{matrix} d \\ \\ c \end{matrix} \!\!\!\!\bigotimes\!\!\!\! \begin{matrix} a \\ \\ b \end{matrix} \;\; \rightarrow \;\; -\frac{i}{s_{ab} s_{bc}} \,. \qquad (3.14)$$

The solid lines are used to indicate that it does not matter whether the states are vectors or hypermultiplets. For each amplitude there is now an additional factor:

$\langle ab \rangle [\overline{cd}]$ for the left-hand side of the cut, and $\langle ef \rangle [\overline{gh}]$ for the right-hand side. This gives a numerator contribution depending on the particle content:

$$\text{(diagram)} \;\to\; \langle ab \rangle [cd] \,, \tag{3.15a}$$

$$\text{(diagram)} \;\to\; \langle a|c|b] \,, \tag{3.15b}$$

$$\text{(diagram)} \;\to\; s_{ac} = s_{bd} \,, \tag{3.15c}$$

where the ordering of legs is irrelevant. When gluing two tree-level amplitudes, we multiply by

$$\text{(diagram)} \;\to\; s_{l_1 l_2} \,, \tag{3.16}$$

where again the type of particles is irrelevant. Finally, the leftover $[qr]\langle \overline{st} \rangle$, as well as the poles in s_{qr} and s_{st}, yield an overall factor depending on the configuration of the four external legs:

$$\text{(diagram)} \;\to\; [qr]\langle st \rangle \hat{\kappa}_{(qr)(qr)} \,, \tag{3.17a}$$

$$\text{(diagram)} \;\to\; [q|s|r\rangle \hat{\kappa}_{(qs)(qt)} \,, \tag{3.17b}$$

$$\text{(diagram)} \;\to\; s_{rt}\hat{\kappa}_{(qs)(rt)} = s_{qs}\hat{\kappa}_{(qs)(rt)} \,, \tag{3.17c}$$

where we have introduced

$$\hat{\kappa}_{(qr)(st)} \equiv \frac{\kappa_{(qr)(st)}}{s_{qr}s_{st}} \,. \tag{3.18}$$

This completes the set of rules required to assemble any cut obtained by gluing four-point amplitudes.

3.2.2 Derivation of $\mathcal{N} = 2$ diagrammatic rules

A convenient way to derive the recursion formula given in eq. (3.12) is by treating chiral and anti-chiral superspace coordinates democratically. We begin with

$$\int d^4 \eta_{l_1} d^4 \eta_{l_2} \kappa^{(\mathrm{L})}_{(ab)(cd)} \kappa^{(\mathrm{R})}_{(ef)(gh)} = [l_1 l_2]^2 \langle ab \rangle \langle cd \rangle \langle ef \rangle \langle gh \rangle [qr][st] \frac{\kappa_{(qr)(st)}}{s_{qr}s_{st}} \,, \tag{3.19a}$$

$$\int d^4 \bar{\eta}_{l_1} d^4 \bar{\eta}_{l_2} \bar{\kappa}^{(\mathrm{L})}_{(\overline{ab})(\overline{cd})} \bar{\kappa}^{(\mathrm{R})}_{(\overline{ef})(\overline{gh})} = \langle l_1 l_2 \rangle^2 [\overline{ab}][\overline{cd}][\overline{ef}][\overline{gh}] \langle \overline{qr} \rangle \langle \overline{st} \rangle \frac{\bar{\kappa}_{(\overline{qr})(\overline{st})}}{s_{\overline{qr}}s_{\overline{st}}} \,, \tag{3.19b}$$

which are CPT conjugates of each other; the former is proved in appendix A. The Fourier transform (2.13) that brings the second expression back into the chiral superspace amounts to replacing

$$\bar{\kappa}_{(\overline{qr})(\overline{st})} \to \kappa_{(qr)(st)} \,, \tag{3.20}$$

which reflects the equivalence of four-point MHV and $\overline{\text{MHV}}$ amplitudes. As $s_{qr} = s_{\overline{qr}}$, $s_{st} = s_{\overline{st}}$ by momentum conservation, this implies that the strings of spinor-helicity brackets are equal across the two formulas.

We can therefore treat chiral and anti-chiral spinor variables democratically. This is naturally accomplished using a square root:

$$
\begin{aligned}
\int \mathrm{d}^4\eta_{l_1} \mathrm{d}^4\eta_{l_2} \kappa^{(\mathrm{L})}_{(ab)(cd)} \kappa^{(\mathrm{R})}_{(ef)(gh)} \\
= s_{l_1 l_2} \left(\langle ab\rangle[\overline{ab}]\langle cd\rangle[\overline{cd}]\langle ef\rangle[\overline{f}]\langle gh\rangle[\overline{gh}][qr]\langle\overline{qr}\rangle[st]\langle\overline{st}\rangle \right)^{\frac{1}{2}} \frac{\kappa_{(qr)(st)}}{s_{qr}s_{st}} ,
\end{aligned}
\tag{3.21}
$$

where the sign is left ambiguous. The last step is to show that, for the left-hand tree amplitude, $\langle ab\rangle[\overline{cd}] = \pm[\overline{ab}]\langle cd\rangle$; this follows by examination for the three possible external helicity configurations listed in the diagrammatic rules (3.15). A similar identity holds for the right-hand side, $\langle ef\rangle[\overline{gh}] = \pm[\overline{ef}]\langle gh\rangle$, and for the external configuration, $\langle\overline{qr}\rangle[st] = \pm[qr]\langle\overline{st}\rangle$. Using these identities we can eliminate the square root, yielding the iterative formula (3.12).

3.2.3 Locality

An important property of the recursive formula (3.12) is that unphysical poles cancel between successive iterations. Suppose we glued a third tree amplitude, with external states encoded by $\kappa^{(\mathrm{X})}_{(ij)(kl)}$. The additional rung carries two new loop momenta l_3 and l_4, where the orientation is irrelevant. Using $\kappa_{(qr)(st)}$ to denote the new external state configuration, we can write

$$
\begin{aligned}
\int \mathrm{d}^4\eta_{l_1} \mathrm{d}^4\eta_{l_2} \mathrm{d}^4\eta_{l_3} \mathrm{d}^4\eta_{l_4} \kappa^{(\mathrm{L})}_{(ab)(cd)} \kappa^{(\mathrm{R})}_{(ef)(gh)} \kappa^{(\mathrm{X})}_{(ij)(kl)} \\
= s_{l_1 l_2} \frac{\langle ab\rangle[\overline{cd}]\langle ef\rangle[\overline{gh}][wx]\langle\overline{yz}\rangle}{s_{wx}s_{yz}} \int \mathrm{d}^4\eta_{l_3} \mathrm{d}^4\eta_{l_4} \kappa^{(\mathrm{L+R})}_{(wx)(yz)} \kappa^{(\mathrm{X})}_{(ij)(kl)} \\
= s_{l_1 l_2} \frac{\langle ab\rangle[\overline{cd}]\langle ef\rangle[\overline{gh}][wx]\langle\overline{yz}\rangle}{s_{wx}s_{yz}} s_{l_3 l_4} \langle wx\rangle[\overline{yz}]\langle ij\rangle[\overline{kl}][qr]\langle\overline{st}\rangle \frac{\kappa_{(qr)(st)}}{s_{qr}s_{st}} \\
= s_{l_1 l_2} s_{l_3 l_4} \langle ab\rangle[\overline{cd}]\langle ef\rangle[\overline{gh}]\langle ij\rangle[\overline{kl}][qr]\langle\overline{st}\rangle \frac{\kappa_{(qr)(st)}}{s_{qr}s_{st}} ,
\end{aligned}
\tag{3.22}
$$

having used $s_{wx} = s_{\overline{yz}}$. We are left only with the poles of the external state configuration, s_{qr} and s_{st}. The above expression is consistent with the diagrammatic rules given in section 3.2.1.

The upshot is that all poles are handled transparently. Physical poles coming from the trees are directly accommodated for by the first rule (3.14); the only other poles are those associated with the external rule (3.17), and which we absorb into $\hat{\kappa}_{(qr)(st)} \equiv \kappa_{(qr)(st)}/(s_{qr}s_{st})$. They are relics of the spinor-helicity notation, arising from the representation of four-dimensional gluon polarization vectors in terms of

spinor-helicity brackets (see e.g. refs. [54, 90]):

$$\varepsilon_+^\mu(p;q) = \frac{[p|\sigma^\mu|q\rangle}{\sqrt{2}\langle qp\rangle}\,, \qquad \varepsilon_-^\mu(p;q) = \frac{[q|\sigma^\mu|p\rangle}{\sqrt{2}[pq]}\,. \qquad (3.23)$$

As we will see in the generalization to three-particle cuts (and higher), at two loops these are the only non-physical poles. Consequently, they are the only poles allowed in a local representation of the integrand.

3.2.4 Off-shell continuation

Our ability to control the physical pole structure of cuts allows us to guess expressions for individual numerators: we lift Lorentz-invariant terms off shell, then attach them to numerators of graphs with the corresponding pole structure. Strings of spinor-helicity brackets arrange themselves into Lorentz inner products and Dirac traces:

$$[i_1 i_2]\langle i_2 i_3\rangle \cdots [i_{k-1} i_k]\langle i_k i_1\rangle = p_{i_1}^{\mu_1} p_{i_2}^{\mu_2} \cdots p_{i_k}^{\mu_k} \operatorname{tr}(\bar{\sigma}_{\mu_1}\sigma_{\mu_2}\cdots\sigma_{\mu_k}) = \operatorname{tr}_+(i_1 i_2 \cdots i_k)\,,$$
$$\langle i_1 i_2\rangle [i_2 i_3] \cdots \langle i_{k-1} i_k\rangle [i_k i_1] = p_{i_1}^{\mu_1} p_{i_2}^{\mu_2} \cdots p_{i_k}^{\mu_k} \operatorname{tr}(\sigma_{\mu_1}\bar{\sigma}_{\mu_2}\cdots\bar{\sigma}_{\mu_k}) = \operatorname{tr}_-(i_1 i_2 \cdots i_k)\,, \qquad (3.24)$$

where $\operatorname{tr}_\pm(i_1 i_2 \cdots i_k) = \frac{1}{2}\operatorname{tr}((1 \pm \gamma_5)i_1 i_2 \cdots i_k)$, and $\operatorname{tr}_\pm(ij) = s_{ij}$. In contrast to the rung rule for $\mathcal{N} = 4$ SYM, the cut structure often leads to triangular subgraphs, enabled by the cut structure allowing both s- and t-channel poles to cancel. The off-shell continuation is not unique and will in some cases lead us to several different representations of the same integrand.

Now let us point out some general features of the $\mathcal{N} = 2$ diagrammatic rules that will be reflected in the explicit off-shell numerators in the next sections.

- In case of two adjacent fundamental hypermultiplets (with aligned matter arrows) on one side of a unitarity cut, the four-hyper rule (3.15c) implies a pole cancellation that makes it equivalent to the $\mathcal{N} = 4$ rung rule (3.9):

$$\vcenter{\hbox{}} = \frac{-is_{12}}{s_{12}s_{1(-l_2)}} \times s_{l_1 l_2} \times \vcenter{\hbox{}} = -\frac{is_{12}}{s_{1(-l_2)}} \times \vcenter{\hbox{}}\,, \quad (3.25)$$

where we have ignored the external states to expose the similarity to eq. (3.7). The resulting absence of the triangle-like term happens because the above four-hyper tree amplitude contains a single t-channel diagram.

- In case of adjacent fundamental and anti-fundamental hypermultiplets on one side of a cut, the four-hyper rule (3.15c) gives two contributors:

$$\vcenter{\hbox{}} = i\left(\frac{1}{s_{12}} + \frac{1}{s_{1(-l_2)}}\right) s_{12} \times \vcenter{\hbox{}}\,, \qquad (3.26)$$

which correspond to a box-like and a triangle-like diagrams, with different matter line routings. The fact that they both have equal numerators justifies our use of the two-term identity for off-shell numerators, as introduced in section 2.3.1.

- Finally, our approach implies explicit IR structure for the kinematic numerators. The numerator rule (3.15b) is especially important in this regard, as it can be re-expressed as

$$\ell \downarrow \mathbb{Q}^{a^-}_{b^+} \rightarrow \langle a|\ell|b], \qquad (3.27)$$

The resulting numerators will evidently vanish whenever $\ell \rightarrow 0$, $\ell \rightarrow -p_a$, or $\ell \rightarrow p_b$, which correspond to the soft regions of loop integration. The numerators will also vanish in the collinear regions where ℓ becomes collinear to p_a or p_b. Such behavior makes a lot of sense, as only vectors should give rise to soft and collinear divergences in the loop integrals, not hypermultiplets (which in our case are also massless) — see e.g. refs. [103–105]. As we shall see (here and in future work currently in progress), this vanishing of the numerators in specific regions serves to block potentially singular regions arising for the hypers.

4 One-loop examples

To illustrate the iterative method of calculating cuts in $\mathcal{N} = 2$ SYM, we begin by considering all three four-point one-loop amplitudes in the MHV sector: with zero, one, and two external hypermultiplet pairs. In each case, the formation of the four-dimensional cuts tells us what structure we should expect in the off-shell numerators, and we find it unnecessary to use ansätze. A complete listing of the non-zero numerators for all three solutions is provided in appendix B.

Given our desire to regulate integrals in $D = 4-2\epsilon$ dimensions, it is also necessary for us to obtain unitarity cuts from higher-dimensional trees. As explained in ref. [66], a convenient method is to calculate cuts arising from the tree amplitudes of six-dimensional $\mathcal{N} = (1,0)$ SYM — the dimensional uplift of four-dimensional $\mathcal{N} = 2$ — using the six-dimensional spinor-helicity formalism [106–112]. One restricts the six-dimensional external momenta to a four-dimensional subspace, and re-interprets the extra two loop momentum components as complex masses: $\mu^2 = \bar{\ell}^2 - \ell^2$, where $\bar{\ell}$ is the four-dimensional part of ℓ.

From these six-dimensional cuts, terms proportional to μ^2 are found by subtracting the previously obtained four-dimensional cuts. These terms are sufficiently simple that they can be lifted off shell without interference to the color-kinematic structure of the four-dimensional numerators. We use a D-dimensional Clifford algebra to write Dirac traces involving ℓ [113, 114]; $\mathrm{tr}_\pm$ are defined in terms of $\gamma_5 = i\gamma^0\gamma^1\gamma^2\gamma^3$, which anticommutes with elements of the four-dimensional subalgebra but commutes with the rest.[6] Computing six-dimensional cuts also provides a check on all of the four-dimensional cuts computed in this paper.

---

[6] A recent review of dimensional-regularization schemes was given in ref. [115].

4.1 External vectors

The one-loop amplitudes with four external vector multiplets, previous versions of which have been obtained in refs. [64, 65, 68, 116–118], are particularly simple to determine. An $\mathcal{N} = 4$ matching identity (see section 2.3.4) relates the pure-adjoint box numerator to the fundamental:

$$n^{[\mathcal{N}=4]}\left(\begin{array}{c} 4 \quad 1 \\ \\ 3 \quad 2 \end{array}\right) = n\left(\begin{array}{c} 4 \quad 1 \\ \\ 3 \quad 2 \end{array}\right) + n\left(\begin{array}{c} 4 \quad 1 \\ \\ 3 \quad 2 \end{array}\right) + n\left(\begin{array}{c} 4 \quad 1 \\ \\ 3 \quad 2 \end{array}\right), \qquad (4.1)$$

where the $\mathcal{N} = 4$ box numerator is given by κ and can be rewritten as

$$n^{[\mathcal{N}=4]}\left(\begin{array}{c} 4 \quad 1 \\ \\ 3 \quad 2 \end{array}\right) = s^2(\hat{\kappa}_{12} + \hat{\kappa}_{34}) + t^2(\hat{\kappa}_{23} + \hat{\kappa}_{14}) + u^2(\hat{\kappa}_{13} + \hat{\kappa}_{24}). \qquad (4.2)$$

All possible combinations of external $\mathcal{N} = 2$ vector multiplets are projected out of κ as coefficients of $\hat{\kappa}_{ij} = \kappa_{ij}/s_{ij}^2$. The fundamental box is the only master — from it we can uniquely fix all other numerators.

We isolate this box numerator from the following family of four-dimensional cuts, determined using the diagrammatic rules given in section 3.2.1. Negative helicities are placed on different external legs to yield coefficients of different $\hat{\kappa}_{ij}$:

$$\begin{array}{c} 4^+ \quad 1^- \\ l_2 \uparrow \qquad \downarrow l_1 \\ 3^+ \quad 2^- \end{array} = 0, \qquad (4.3a)$$

$$\begin{array}{c} 4^+ \quad 1^- \\ l_2 \uparrow \qquad \downarrow l_1 \\ 3^- \quad 2^+ \end{array} = -\frac{\langle 3|l_2|4]}{s\, l_2^2} \times s \times \frac{\langle 1|l_1|2]}{s\, l_1^2} \times [13]\langle 24\rangle \hat{\kappa}_{13} = \frac{\text{tr}_-(1l_1 24 l_2 3)}{s\, l_1^2 l_2^2}\hat{\kappa}_{13}, \quad (4.3b)$$

$$\begin{array}{c} 4^- \quad 1^- \\ l_2 \uparrow \qquad \downarrow l_1 \\ 3^+ \quad 2^+ \end{array} = -\frac{[3|l_2|4\rangle}{s\, l_2^2} \times s \times \frac{\langle 1|l_1|2]}{s\, l_1^2} \times [14]\langle 23\rangle \hat{\kappa}_{14} = \frac{\text{tr}_-(1l_1 23 l_2 4)}{s\, l_1^2 l_2^2}\hat{\kappa}_{14}. \quad (4.3c)$$

The box is separated from the triangles and bubbles which also contribute by further cutting into the l_1 and l_2 propagators; in that case $\text{tr}_\pm(1l_1 24 l_2 3) = -s\,\text{tr}_\pm(1l_1 l_2 3)$ and $\text{tr}_\pm(1l_1 23 l_2 4) = 0$. The $\hat{\kappa}_{23}$, $\hat{\kappa}_{24}$, and $\hat{\kappa}_{34}$ coefficients are related by CPT conjugation; the descendants are determined using commutation relations:

$$n\left(\begin{array}{c} 4 \quad \overset{\ell}{\rightarrow} \quad 1 \\ \\ 3 \quad 2 \end{array}\right) = \hat{\kappa}_{13}\,\text{tr}_-(1(\ell - p_1)(\ell + p_4)3) + \hat{\kappa}_{24}\,\text{tr}_+(1(\ell - p_1)(\ell + p_4)3) \qquad (4.4a)$$
$$+ \mu^2\big(s(\hat{\kappa}_{12}+\hat{\kappa}_{34}) + t(\hat{\kappa}_{23}+\hat{\kappa}_{14}) + u(\hat{\kappa}_{13}+\hat{\kappa}_{24})\big),$$

$$n\left(\begin{array}{c} 1 \quad 2 \\ \ell \uparrow \\ 4 \quad 3 \end{array}\right) = (\hat{\kappa}_{13} + \hat{\kappa}_{34})\,\text{tr}_-(1(\ell - p_1)(\ell + p_4)3) \qquad (4.4b)$$
$$+ (\hat{\kappa}_{12} + \hat{\kappa}_{24})\,\text{tr}_+(1(\ell - p_1)(\ell + p_4)3) + (\hat{\kappa}_{12} + \hat{\kappa}_{34})t\ell^2,$$

$$n\left(\begin{array}{c} 4 \quad \overset{\ell}{\rightarrow} \quad 1 \\ \\ 3 \quad 2 \end{array}\right) = 2\ell\cdot(p_{12} - \ell)[t(\hat{\kappa}_{23} + \hat{\kappa}_{14}) - u(\hat{\kappa}_{13} + \hat{\kappa}_{24})], \qquad (4.4c)$$

Figure 1: The three one-loop masters with mixed external particle content.

By resubstituting back into the cuts given in eq. (4.3), we confirm the color duality of these kinematic numerators.[7]

Box numerators involving four-term traces of this kind have previously appeared in the context of D-dimensional local integrands [80, 119]. A box integral with numerator $\mathrm{tr}_\pm[1(\ell - p_1)(\ell + p_4)3]$ was there found to be free of both UV and IR divergences — in fact, it is proportional to the $(D+2)$-dimensional scalar box integral, which does not diverge. The mechanism blocking these divergences was discussed at the end of section 3.2.4: when ℓ enters any potentially soft or collinear region, vanishing of the trace blocks the divergence. The descendants have similar properties, so these are our first examples of numerators with an IR structure that manifests vanishing of soft and collinear limits of matter-line momenta.

4.2   External vectors + matter

There are three masters, drawn in figure 1. We examine the first on its s-channel cut:

$$\text{(diagram)} = \frac{\mathrm{tr}_+(4l_1l_2l_112)}{s\,s_{4l_1}s_{2l_2}}\hat{\kappa}_{(12)(13)} = -\frac{\mathrm{tr}_+(4l_112)}{s_{4l_1}s_{2l_2}}\hat{\kappa}_{(12)(13)}\,, \qquad (4.5)$$

where the Dirac algebra is used to cancel the s-channel pole. This implies that, similar to the rung rule in $\mathcal{N}=4$ SYM, there are no triangles; only the first box drawn in figure 1 contributes. The second and third masters are isolated on near-identical cuts: the former by exchanging $p_3 \leftrightarrow p_4$, and the latter by also exchanging $p_1 \leftrightarrow p_2$. As the diagrammatic rules for the numerators do not depend on the ordering of the tree amplitudes (except for relabeling) the same result is obtained.

---

[7]There are other descendants with bubbles on external legs or tadpoles, listed in appendix B. However, as explained in ref. [66], these contributions vanish upon integration as they lack a proper mass scale.

The three masters are

$$n\left(\begin{array}{c}\text{[diagram]}\end{array}\right) = \mathrm{tr}_+(4\ell12)\hat{\kappa}_{(12)(13)} + \mathrm{tr}_-(4\ell12)\hat{\kappa}_{(24)(34)}\,, \tag{4.6a}$$

$$n\left(\begin{array}{c}\text{[diagram]}\end{array}\right) = \mathrm{tr}_+(3\ell12)\hat{\kappa}_{(12)(14)} + \mathrm{tr}_-(3\ell12)\hat{\kappa}_{(23)(34)}\,, \tag{4.6b}$$

$$n\left(\begin{array}{c}\text{[diagram]}\end{array}\right) = \mathrm{tr}_+(3\ell21)\hat{\kappa}_{(12)(24)} + \mathrm{tr}_-(3\ell21)\hat{\kappa}_{(13)(34)}\,, \tag{4.6c}$$

where in all three cases the coefficient of tr_- is related by CPT conjugation. It can be checked using six-dimensional cuts that continuation to $D = 4 - 2\epsilon$ does not introduce terms proportional to μ^2; this can also be argued from the absence of quadratic ℓ terms in the numerators.

As further confirmation of these expressions we can also examine the t-channel cuts. The first master contributes to

$$\text{[diagram]} = -\left(\frac{1}{t} + \frac{1}{l_2^2}\right)\frac{\mathrm{tr}_+(4l_112)}{l_1^2}\hat{\kappa}_{(12)(13)}\,. \tag{4.7}$$

In this case there are two contributors; as explained in section 3.2.4, the four-hyper amplitude naturally separates this cut into two contributions with equal numerators:

$$n\left(\begin{array}{c}\text{[diagram]}\end{array}\right) = n\left(\begin{array}{c}\text{[diagram]}\end{array}\right)\,, \tag{4.8}$$

which is a two-term identity (see section 2.3.1). The t-channel cut for the second master is redundant as it related by symmetry to the s-channel one. For the third master, it gives

$$\text{[diagram]} = \text{[diagram]} \quad \text{[diagram]} = -\left(\frac{\mathrm{tr}_+(12l_13)}{l_1^2 l_2^2} - \frac{2\,\mathrm{tr}_+(12l_23)}{t\, l_2^2}\right)\hat{\kappa}_{(12)(24)}\,. \tag{4.9}$$

We are required to sum over the two possible helicity configurations, and the Dirac algebra is used to expose the two contributors: the box and another triangle. They are automatically related by a commutation relation:

$$n\left(\begin{array}{c}\text{[diagram]}\end{array}\right) = n\left(\begin{array}{c}\text{[diagram]}\end{array}\right) - n\left(\begin{array}{c}\text{[diagram]}\end{array}\right)$$

$$= -2\,\mathrm{tr}_+(4\ell12)\hat{\kappa}_{(12)(13)} - 2\,\mathrm{tr}_-(4\ell12)\hat{\kappa}_{(24)(34)}\,. \tag{4.10}$$

This completes the set of non-zero numerators, which are also listed in appendix B.2; all of the extra off-shell identities described in section 2.3 are satisfied by these numerators including $\mathcal{N} = 4$ matching identities:

$$n\left(\text{diagram}\right) + n\left(\text{diagram}\right) = su(\hat{\kappa}_{(12)(13)} + \hat{\kappa}_{(24)(34)}),\qquad(4.11\text{a})$$

$$n\left(\text{diagram}\right) + n\left(\text{diagram}\right) = st(\hat{\kappa}_{(12)(14)} + \hat{\kappa}_{(23)(34)}),\qquad(4.11\text{b})$$

$$n\left(\text{diagram}\right) + 2n\left(\text{diagram}\right) = 0.\qquad(4.11\text{c})$$

These numerators have good IR behavior — taking the loop momentum associated with an edge carrying hypermultiplets in any one of them to zero, the numerator does indeed vanish; this does not happen for internal gluon lines. This indicates that soft divergences can indeed develop, but only as a result of soft vectors being exchanged, not soft hypers. Collinear divergences can also develop, but only at vertices connecting an internal gluon line.

4.3 External matter

A color-dual representation for four external matter multiplets has previously been obtained in ref. [64] via an orbifold construction.[8] A single master is sufficient; we choose the box numerator contributing to

$$\text{diagram} = -\frac{s^2}{l_1^2 l_2^2}\hat{\kappa}_{(12)(34)}.\qquad(4.12)$$

The box numerator is easily read off as the only contributor, and the full set of numerators for this amplitude is

$$n\left(\text{diagram}\right) = s^2\hat{\kappa}_{(12)(34)},\qquad(4.13\text{a})$$

$$n\left(\text{diagram}\right) = n\left(\text{diagram}\right) = -n\left(\text{diagram}\right)\qquad(4.13\text{b})$$

$$= n\left(\text{diagram}\right) = -\frac{1}{2}n\left(\text{diagram}\right) = -su\hat{\kappa}_{(13)(24)}.$$

In particular, the other box numerator is related by the matter-reversal symmetry identity given in eq. (2.25); the first triangle and first bubble are equated to the

box using two-term identities. Once again, by determining the relevant cuts in $D = 6$ dimensions we have confirmed that these expressions are unmodified by terms proportional to μ^2.

An incongruous feature of these numerators is their soft behavior. Until now, there has been a well-established pattern: when loop momenta carried on hypermultiplet edges go to zero the numerators vanish. This is consistent with the fact that only vector multiplets should give rise to soft regions, not hypermultiplets, as can be seen from the IR factorization formulae [103–105]. Without any loop-momentum dependence in these numerators, this clearly cannot happen.

We therefore question whether one should add loop-momentum-dependent terms vanishing on the s-channel cuts in order to restore this behavior. The statement clarifies further upon examination of a t-channel cut:

$$\text{(diagram)} = \text{(diagram)} + \text{(diagram)} = \frac{2l_1^2 l_2^2 + 2t l_1 \cdot l_2}{t \, l_1^2 l_2^2} s \, \hat{\kappa}_{(12)(34)} . \qquad (4.14)$$

Now from this perspective, a natural suggestion for the two box numerators is

$$n\left(\text{(diagram)}\right) = 2s \, \ell \cdot (p_{12} - \ell) \hat{\kappa}_{(12)(34)} , \qquad (4.15a)$$

$$n\left(\text{(diagram)}\right) = 2u \, \ell \cdot (\ell - p_{12}) \hat{\kappa}_{(13)(24)} , \qquad (4.15b)$$

where the latter is again related to the former by matter-reversal symmetry (2.25). These numerators vanish when $\ell \to 0$ or $\ell \to p_{12}$ and still reduce to the previous expressions (4.13) on the s-channel cuts due to $2\ell \cdot (p_{12} - \ell) = s - \ell^2 - (\ell - p_{12})^2$.

The resulting set of numerators satisfies the cuts conditions, color-kinematics duality and the two-term identities but violates the $\mathcal{N} = 4$ matching conditions. Moreover, an unfortunate consequence of the above numerator rearrangement is that the descendants become both numerous and more complicated (for instance, there are now non-vanishing bubbles and tadpoles). This suggests that, should one wish to expose the IR behavior in this way, maintaining manifest color-kinematics duality is not always the best approach. Nevertheless, when scattering four hypermultiplets at two loops we will find that such rearrangements become necessary in order to obtain valid color-dual numerators.

5 Two-loop examples

We now proceed to the main result of this paper: the complete set of two-loop four-point MHV amplitudes in $\mathcal{N} = 2$ SQCD. A color-dual representation of the

Figure 2: Three two-loop masters with four external vector multiplets.

amplitude with four external vector multiplets was already found in ref. [66] — in fact, two solutions were found which emphasized different physical properties. We begin by re-deriving one of these two solutions from iterative two-particle cuts; when expressed in terms of Dirac traces, the resulting solution is written far more compactly than as originally presented. We then proceed to calculate the two-loop amplitudes with one and two external hypermultiplet pairs.

As we explained at one loop, using cuts in strictly four dimensions misses extra-dimensional terms $\mu_{ij} = \bar{\ell}_i \cdot \bar{\ell}_j - \ell_i \cdot \ell_j$ needed for dimensional regularization ($\bar{\ell}_i$ is the four-dimensional part of ℓ_i). By evaluating cuts in six-dimensional $\mathcal{N} = (1,0)$ SYM we recover the missing terms, which are simple enough not to interfere with the color duality of the four-dimensional numerators (again, see ref. [66] for details). A new feature is the antisymmetric object $\epsilon(\mu_1, \mu_2)$, which is an extra-dimensional echo of the six-dimensional Levi-Civita tensor:

$$\epsilon(\mu_1, \mu_2) = \frac{\epsilon^{(6)}(v_1, v_2, v_3, v_4, \ell_1, \ell_2)}{\epsilon(v_1, v_2, v_3, v_4)}, \tag{5.1}$$

where v_i are four-dimensional vectors. Its appearance is due to the unavoidably chiral nature of certain six-dimensional internal states; although it vanishes upon integration, we keep it here as it gives rise to non-chiral contributions after the double copy: $\epsilon(\mu_1, \mu_2)^2 = \mu_{11}\mu_{22} - \mu_{12}^2$.

5.1 External vectors

First we summarize the main result of ref. [66], updating the notation as necessary to make use of Dirac traces. The solution we are interested in was chosen to satisfy two-term and $\mathcal{N} = 4$ identities, as well as matter-reversal symmetry and CPT conjugation. A suitable choice of three masters is displayed in figure 2. The pentagon triangle vanishes on its maximal cut; by setting it to zero, while demanding locality of all numerators, it was found that the other two masters are uniquely fixed. This left a total of 19 non-zero numerators.

The $\mathcal{N} = 4$ identities are particularly useful, as they ensure that all numerators with pure-adjoint content (no hyper loops) can be uniquely written in terms of those with internal hyper loops using $\mathcal{N} = 4$ identities. There are only two non-zero two-loop four-point $\mathcal{N} = 4$ SYM numerators in the MHV sector:

$$n^{[\mathcal{N}=4]}\left(\begin{matrix}\text{\tiny diagram}\end{matrix}\right) = n^{[\mathcal{N}=4]}\left(\begin{matrix}\text{\tiny diagram}\end{matrix}\right) = s\sum_{i<j}\kappa_{ij}, \tag{5.2}$$

where the $\mathcal{N} = 2$ content has been projected out. Using the two-term identities, any numerator with two hypermultiplet loops can be uniquely specified in terms of one with a single loop. So only numerators with a single hypermultiplet loop need to be specified — there are 10 of these.

Up to relabeling of loop momenta and overall constants, four are equal:[9]

$$n\left(\vcenter{\hbox{}}\right) = n\left(\vcenter{\hbox{}}\right) = n\left(\vcenter{\hbox{}}\right) = -\frac{1}{2}n\left(\vcenter{\hbox{}}\right)$$

$$= \hat{\kappa}_{13}\,\mathrm{tr}_-(1\ell_1 24\ell_2 3) + \hat{\kappa}_{14}\,\mathrm{tr}_-(1\ell_1 23\ell_2 4) + \hat{\kappa}_{23}\,\mathrm{tr}_+(1\ell_1 23\ell_2 4) + \hat{\kappa}_{24}\,\mathrm{tr}_+(1\ell_1 24\ell_2 3)$$
$$- s\mu_{12}\left(s(\hat{\kappa}_{12} + \hat{\kappa}_{34}) + t(\hat{\kappa}_{23} + \hat{\kappa}_{14}) + u(\hat{\kappa}_{13} + \hat{\kappa}_{24})\right)$$
$$+ i\epsilon(\mu_1, \mu_2)s^2(\hat{\kappa}_{12} - \hat{\kappa}_{34})\,. \tag{5.3}$$

There is another non-planar double box with a similar structure, given by

$$n\left(\vcenter{\hbox{}}\right) = s(\hat{\kappa}_{12}\,\mathrm{tr}_+(3\ell_{12}\ell_2 4) + \hat{\kappa}_{34}\,\mathrm{tr}_-(3\ell_{12}\ell_2 4))$$
$$+ \hat{\kappa}_{13}\,\mathrm{tr}_-(1\ell_2 42\ell_{12}3) + \hat{\kappa}_{23}\,\mathrm{tr}_+(1\ell_{12}32\ell_2 4)$$
$$+ \hat{\kappa}_{14}\,\mathrm{tr}_-(1\ell_{12}32\ell_2 4) + \hat{\kappa}_{24}\,\mathrm{tr}_+(1\ell_2 42\ell_{12}3)$$
$$+ s(\mu_{12} + \mu_{22})[s(\hat{\kappa}_{12} + \hat{\kappa}_{34}) + t(\hat{\kappa}_{23} + \hat{\kappa}_{14}) + u(\hat{\kappa}_{13} + \hat{\kappa}_{24})]$$
$$+ i\epsilon(\mu_1, \mu_2)[t^2(\hat{\kappa}_{23} - \hat{\kappa}_{14}) + u^2(\hat{\kappa}_{13} - \hat{\kappa}_{24})]\,, \tag{5.4}$$

where $\ell_{12} = \ell_1 + \ell_2$. The only non-zero pentagon triangle with internal matter is

$$n\left(\vcenter{\hbox{}}\right) = - s(\hat{\kappa}_{12}\,\mathrm{tr}_+(3\ell_{12}\ell_2 4) + \hat{\kappa}_{34}\,\mathrm{tr}_-(3\ell_{12}\ell_2 4))$$
$$- t(\hat{\kappa}_{23}\,\mathrm{tr}_+(1\ell_{12}\ell_2 4) + \hat{\kappa}_{14}\,\mathrm{tr}_-(1\ell_{12}\ell_2 4))$$
$$- u(\hat{\kappa}_{13}\,\mathrm{tr}_+(2\ell_{12}\ell_2 4) + \hat{\kappa}_{24}\,\mathrm{tr}_-(2\ell_{12}\ell_2 4))$$
$$- i\epsilon(\mu_1, \mu_2)[s^2(\hat{\kappa}_{12} - \hat{\kappa}_{34}) + t^2(\hat{\kappa}_{23} - \hat{\kappa}_{14}) + u^2(\hat{\kappa}_{13} - \hat{\kappa}_{24})]\,, \tag{5.5}$$

Finally, the other four non-zero numerators are

$$n\left(\vcenter{\hbox{}}\right) = -2\ell_1 \cdot \ell_2 \sum_{i<j} \kappa_{ij}\,, \qquad n\left(\vcenter{\hbox{}}\right) = -4\ell_1 \cdot \ell_2 \sum_{i<j} \kappa_{ij}\,,$$

$$n\left(\vcenter{\hbox{}}\right) = 2\ell_2 \cdot (p_4 - \ell_2) \sum_{i<j} \kappa_{ij}\,, \qquad n\left(\vcenter{\hbox{}}\right) = 4\ell_2 \cdot p_4 \sum_{i<j} \kappa_{ij}\,. \tag{5.6}$$

As explained in ref. [66], the three diagrams with bubbles on external legs or tadpoles (5.6) are of no concern as they vanish upon integration.

---

[9] In this section we use both κ_{ab} and $\hat{\kappa}_{ab} \equiv \hat{\kappa}_{(ab)(ab)} = \kappa_{(ab)}/s_{ab}^2$ to our convenience.

This solution has good soft behavior: setting the loop momentum of any internal edge carrying hypermultiplets to zero, the corresponding numerator vanishes. In fact, double-box integrals involving the six-term traces appearing in eq. (5.3) have already been calculated by Caron-Huot and Larsen [120]; they were suggested as forming part of a basis of IR-finite integrals. From their results, we conclude that the integral of the first double box with hypermultiplets circulating the outside edge is both UV and IR finite to all orders in ϵ.

To see how the solution arises, we strategically choose cuts to yield information about the non-vanishing masters. Beginning with the first double box, we consider

$$\text{(diagram)} = 0\,, \tag{5.7a}$$

$$\text{(diagram)} = \left(\frac{1}{s} + \frac{1}{l_3^2}\right) \frac{\text{tr}_-(1l_124l_23)}{l_1^2 l_2^2} \hat{\kappa}_{13}\,, \tag{5.7b}$$

$$\text{(diagram)} = \left(\frac{1}{s} + \frac{1}{l_3^2}\right) \frac{\text{tr}_-(1l_123l_24)}{l_1^2 l_2^2} \hat{\kappa}_{14}\,. \tag{5.7c}$$

These are almost identical to the one-loop cuts with four external vectors given in eq. (4.3); the new feature is the central tree amplitude insertion which, as explained in section 3.2.4, naturally implies two numerators equated by a two-term identity:

$$n\left(\text{(diagram)}\right) = n\left(\text{(diagram)}\right)\,. \tag{5.8}$$

The double box can also be isolated from the double triangle on

$$\text{(diagram)} = 0\,, \tag{5.9a}$$

$$\text{(diagram)} = -\frac{\langle 3|l_2|4]}{(l_2+p_4)^2(l_2-p_3)^2} \times s \times \frac{\langle 1|l_1|2]}{s\,l_1^2} \times [13]\langle 24\rangle \hat{\kappa}_{13}$$
$$= \frac{\text{tr}_-(1l_124l_23)}{l_1^2(l_2+p_4)^2(l_2-p_3)^2}\hat{\kappa}_{13}\,, \tag{5.9b}$$

$$\text{(diagram)} = -\frac{\langle 4|l_2|3]}{(l_2+p_4)^2(l_2-p_3)^2} \times s \times \frac{\langle 1|l_1|2]}{s\,l_1^2} \times [14]\langle 23\rangle \hat{\kappa}_{14}$$
$$= \frac{\text{tr}_-(1l_123l_24)}{l_1^2(l_2+p_4)^2(l_2-p_3)^2}\hat{\kappa}_{14}\,. \tag{5.9c}$$

In the second two cases, we have re-used the one-loop cut given in eq. (4.5) for the two amplitudes on the left-hand side — we simply stripped away the part of the expression given by the external rules. So only the double box contributes, and we

Figure 3: The two two-loop masters with external hypermultiplets.

reproduce the same expression. We are also reminded that the pentagon triangle can safely be set to zero.

Finally, the other double box can be determined from

$$\text{(diagram)} = 0\,, \tag{5.10a}$$

$$\text{(diagram)} = -\frac{\operatorname{tr}_-(1l_124l_33)}{l_1^2 l_2^2 l_3^2}\hat{\kappa}_{13} - \frac{2\operatorname{tr}_-(1l_124l_23)}{s\,l_1^2 l_2^2}\hat{\kappa}_{13}\,, \tag{5.10b}$$

$$\text{(diagram)} = -\frac{\operatorname{tr}_-(1l_123l_34)}{l_1^2 l_2^2 l_3^2}\hat{\kappa}_{14} - \frac{2\operatorname{tr}_-(1l_123l_24)}{s\,l_1^2 l_2^2}\hat{\kappa}_{14}\,, \tag{5.10c}$$

This time we re-used the one-loop cut given in eq. (4.9), saving us the need to sum over helicity configurations of the vector multiplets. The two contributing numerators, a double box and double triangle, are related by a commutation relation:

$$n\left(\text{(diagram)}\right) = n\left(\text{(diagram)}\right) - n\left(\text{(diagram)}\right)\,. \tag{5.11}$$

This works by precise analogy to the one-loop relation given in eq. (4.10).

5.2 External matter

In this case, assuming that the matter-reversal symmetry discussed in section 2.3.3 holds for non-tadpole diagrams, there are two masters displayed in figure 3. The first is most naturally isolated from

$$\text{(diagram)} = \frac{s^3}{l_1^2 l_2^2 l_3^2}\hat{\kappa}_{(12)(34)}\,. \tag{5.12}$$

We encountered a similar pattern when dealing with four external hypermultiplets at one loop (4.12), and there it was simple to read off a color-dual box numerator. As explained in section 3.2.4, the new tree amplitude insertion implies that the double box should be given by a rung rule from the first box numerator in eq. (4.13), so in this case simply $s^3\hat{\kappa}_{(12)(34)}$.

Unfortunately, we have confirmed by direct calculation that such a choice is incompatible with a color-dual representation of the complete amplitude assuming
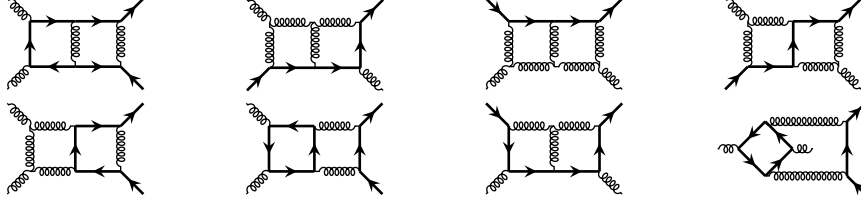
Figure 4: Two-loop masters with two external vector and matter multiplets.

two-term identities. From the one-loop discussion in section 4.3 we learned that there is a second solution if we change the off-shell continuation to carry loop momenta. Converting one factor of s into $2\,(l_1+p_1)\cdot(p_2-l_1)$ or $2\,(l_2+p_4)\cdot(p_3-l_2)$ inside eq. (5.12), we make the following simple ansatz for the numerator:

$$n\left(\begin{array}{c}4\\ \ell_2\downarrow\\ 3\end{array}\begin{array}{c}\\ \end{array}\begin{array}{c}1\\ \downarrow\ell_1\\ 2\end{array}\right) = s^2\left[c_1 s + c_2(\ell_1 + p_1)\cdot(\ell_1 - p_2) + c_3(\ell_2 + p_4)\cdot(\ell_2 - p_3)\right]\hat{\kappa}_{(12)(34)}\,,$$

(5.13)

where c_i are numerical coefficients to be determined. The same terms are also suggested by cuts of the form

$$\begin{array}{c}4\\ 3\end{array}\begin{array}{c}\\ \end{array}\begin{array}{c}1\\ 2\end{array}\,,\qquad\qquad \begin{array}{c}4\\ 3\end{array}\begin{array}{c}\\ \end{array}\begin{array}{c}1\\ 2\end{array}\,,\qquad (5.14)$$

which can again be obtained by recycling the one-loop results.

The situation is even more difficult for the second master in figure 3. The three cuts above naturally propose the same off-shell continuation, which does not conform to a color-dual representation (assuming two-term identities), as we explicitly checked. We therefore use an ansatz construction for this master along the lines of ref. [66]. It is, however, simplified by the diagrammatic rule (3.17c), which suggests an overall factor of s_{ab}, where a and b denote the two external hyper legs. Combining with the ansatz (5.13) and applying the constraints described in section 2.3, we arrive at a solution with a single free parameter. In our final numerators

$$n\left(\begin{array}{c}4\\ \ell_2\downarrow\\ 3\end{array}\begin{array}{c}\\ \end{array}\begin{array}{c}1\\ \downarrow\ell_1\\ 2\end{array}\right) = -s^2\left[(\ell_1 + p_1)\cdot(\ell_1 - p_2) + (\ell_2 + p_4)\cdot(\ell_2 - p_3)\right]\hat{\kappa}_{(12)(34)}\,,\quad (5.15a)$$

$$n\left(\begin{array}{c}4\\ \ell_2\downarrow\\ 3\end{array}\begin{array}{c}\\ \uparrow\ell\\ \end{array}\begin{array}{c}1\\ \downarrow\ell_1\\ 2\end{array}\right) = \frac{1}{2}st\left[(\ell_1 - p_1 - p_3)^2 - 2\,(\ell_2\cdot\ell_3)\right]\hat{\kappa}_{(14)(23)}\,,\qquad (5.15b)$$

we fixed it to have the shortest possible expression for the second master.

5.3 External vectors + matter

The last — and most difficult — two-loop external MHV state configuration is with a single hypermultiplet pair and two vectors of opposite chirality. The number of

masters given in figure 4 is significantly larger than for all the other cases. Similar to what we have seen with four external matter states, a color-dual representation does not always agree with the off-shell continuation suggested by the cuts. Nevertheless, we are able to find a valid color-dual representation for two of the master numerators in figure 4 directly from the cuts. Re-using computations from the corresponding one-loop example, we bring the cuts for these two masters into the form

$$
\begin{aligned}
\text{(5.16a)} \quad &= -\frac{\text{tr}_-(4l_231)(s+l_3^2)(s+l_1^2)}{sl_1^2l_2^2l_3^2}\hat{\kappa}_{(41)(42)} \\
&\quad -\frac{\text{tr}_+(4l_231)(s+l_3^2)(s+l_1^2)}{sl_1^2l_2^2l_3^2}\hat{\kappa}_{(31)(32)}\,,
\end{aligned}
$$

$$
\text{(5.16b)} \quad = -\frac{\text{tr}_-(4l_231)(s+l_1^2)}{l_1^2l_2^2l_3^2}\hat{\kappa}_{(41)(42)} - \frac{\text{tr}_+(4l_231)(s+l_1^2)}{l_1^2l_2^2l_3^2}\hat{\kappa}_{(31)(32)}\,,
$$

$$
\begin{aligned}
\text{(5.16c)} \quad &= \frac{[s\,\text{tr}_+(3l_341)+2l_3^2\,\text{tr}_+(3l_241)](s+l_1^2)}{sl_1^2l_2^2l_3^2}\hat{\kappa}_{(41)(42)} \\
&\quad + \frac{[s\,\text{tr}_-(3l_341)+2l_3^2\,\text{tr}_-(3l_241)](s+l_1^2)}{sl_1^2l_2^2l_3^2}\hat{\kappa}_{(31)(32)}\,,
\end{aligned}
$$

$$
\text{(5.16d)} \quad = \frac{\text{tr}_+(3l_341)(s+l_1^2)}{l_1^2l_2^2l_3^2}\hat{\kappa}_{(41)(42)} + \frac{\text{tr}_-(3l_341)(s+l_1^2)}{l_1^2l_2^2l_3^2}\hat{\kappa}_{(31)(32)}\,.
$$

This leads us to simple expressions for the corresponding double-box numerators:

$$
n\left(\text{(diagram)} \right) = -s\,\text{tr}_-(4\ell_231)\hat{\kappa}_{(41)(42)} - s\,\text{tr}_+(4\ell_231)\hat{\kappa}_{(31)(32)}\,, \tag{5.17a}
$$

$$
n\left(\text{(diagram)} \right) = s\,\text{tr}_+(3\ell_341)\hat{\kappa}_{(41)(42)} + s\,\text{tr}_-(3\ell_341)\hat{\kappa}_{(31)(32)}\,, \tag{5.17b}
$$

and these do form a valid representation.

The other seven masters fall out of the pattern and had to be computed through an ansatz construction. After implementing as many constraints as possible from section 2.3 the solution contains one free parameter, that we fix by hand to obtain the shortest possible representation. The expressions for all numerators are attached in an ancillary file to the arXiv submission of this paper as discussed in appendix B.

6   Multi-particle cuts

We generalize the recursion to multi-particle cuts, deriving general formulas for cuts of MHV or $\overline{\text{MHV}}$ amplitudes built from MHV and $\overline{\text{MHV}}$ trees. The structure of supersums for less than maximal supersymmetries has previously been studied in ref. [121], using similar on-shell superspace techniques as we will employ here. As

there is no natural generalization of κ at higher points, our generalizations of the $\mathcal{N} = 4$ and $\mathcal{N} = 2$ supersymmetric recursion formulas, given in eqs. (3.3) and (3.12), are built out of full tree-level amplitudes containing physical poles in their Parke-Taylor factors; the resulting cut formulas are therefore less compact. Nevertheless, if the final result is a four-point cut then there is a simple mechanism to reintroduce κ and cancel all unphysical poles. These expressions can be used for an iteration to any loop order.

In order to determine higher-loop or higher-point amplitudes one generally also requires cuts containing non-MHV (and non-$\overline{\text{MHV}}$) amplitudes. However, to obtain two-loop MHV amplitudes this is not necessary; the techniques described here have been used to check the two-loop representations detailed in the previous section.

6.1 $\mathcal{N} = 4$ **SYM**

Consider a cut of the form

$$
\vcenter{\hbox{}} = \int \mathrm{d}^4\eta_{l_1} \cdots \mathrm{d}^4\eta_{l_r} A^{(0)}_{k+m}(1, \ldots, k, l_1, \ldots, l_r) \\
\times A^{(0)}_{n-k+m}(k+1, \ldots, n, -l_m, \ldots, -l_1) \,. \tag{6.1}
$$

We are interested in cuts for which the individual trees and the full external state configuration live in either the MHV or $\overline{\text{MHV}}$ sector. There are two ways this can happen: (i) one of the trees is MHV and the other is $\overline{\text{MHV}}$, in which case we require $k = 2$ or $k = n - 2$; (ii) both trees are MHV or $\overline{\text{MHV}}$, in which case we require $m = 2$ (a two-particle cut). When $k = m = 2$ both cases should reduce to the existing iterated two-particle cuts; for more than a three-particle cut ($m > 3$) this will give only specific contributions to the full cut. We consider the two possibilities in turn.

6.1.1 $\overline{\text{MHV}} \times$ **MHV**

In this configuration the cut (6.1) is given by the superspace integration

$$
\vcenter{\hbox{}} = - \int \mathrm{d}^4\eta_{l_1} \cdots \mathrm{d}^4\eta_{l_m} \frac{\delta^8(\bar{Q}_{\mathrm{L}})}{[12][2\,l_1] \cdots [l_m 1]} \frac{\delta^8(Q_{\mathrm{R}})}{\langle 34 \rangle \cdots \langle n\,l_m \rangle \cdots \langle l_1 3 \rangle} \,, \tag{6.2}
$$

where we have inserted the Parke-Taylor formulas (2.6) and (2.11) for right-hand MHV and left-hand $\overline{\text{MHV}}$ tree amplitudes respectively; using the symmetry between chiral and anti-chiral superspace we can specialize to $k = 2$ without loss of generality. We also implicitly assume a Fourier transform (2.13) of the first delta function to bring it into the chiral superspace.

To see the iterated structure some manipulation is required. The product of the two Parke-Taylor denominators is brought into the form

$$\frac{1}{[12][2l_1]\cdots[l_m1]}\frac{1}{\langle 34\rangle\cdots\langle n\,l_m\rangle\cdots\langle l_1 3\rangle}$$
$$=\frac{\langle 12\rangle}{[12]}\underbrace{\frac{\langle 2|3|l_1|2\rangle\langle 1|l_m|n|1\rangle}{s_{2l_1}s_{l_m1}s_{n(-l_m)}s_{(-l_1)3}s_{l_1l_2}\cdots s_{l_{m-1},l_m}}}_{\text{phys. poles}}\underbrace{\frac{1}{\langle 12\rangle\cdots\langle n1\rangle}}_{\text{Parke-Taylor}}\,,\qquad(6.3)$$

which exposes another Parke-Taylor factor. The overall supersum is given by

$$\int \mathrm{d}^{\mathcal{N}}\eta_{l_1}\cdots \mathrm{d}^{\mathcal{N}}\eta_{l_m}\delta^{2\mathcal{N}}(\bar{Q}_{\mathrm{L}})\delta^{2\mathcal{N}}(Q_{\mathrm{R}})=[12]^{\mathcal{N}}\delta^{2\mathcal{N}}(Q)\,,\qquad(6.4)$$

where Q is the overall supermomentum. Putting the pieces together,

$$\vcenter{\hbox{}}=\frac{i\,s_{12}\,\mathrm{tr}_-(23l_121l_mn1)}{s_{2l_1}s_{(-l_1)3}s_{1l_m}s_{(-l_m)n}s_{l_1l_2}\cdots s_{l_{m-1}\,l_m}}A_n^{(0),\mathrm{MHV}}(1,\ldots,n)\,.\qquad(6.5)$$

Via CPT conjugation the cut with MHV $\leftrightarrow \overline{\mathrm{MHV}}$ is given by replacing $|i\rangle \leftrightarrow |i]$, which exchanges $\mathrm{tr}_+ \leftrightarrow \mathrm{tr}_-$.

If, at the end of several iteration steps, we are left with the cut of a four-point amplitude the result is simplified by reinstating κ:

$$\vcenter{\hbox{}}=-\frac{\mathrm{tr}_-(43l_121l_m)}{s_{2l_1}s_{(-l_1)3}s_{1l_m}s_{(-l_m)4}s_{l_1l_2}\cdots s_{l_{m-1}l_m}}\kappa\,.\qquad(6.6)$$

We recover the two-particle cut (3.5) for $m=2$ using $\mathrm{tr}_-(43l_121l_2)=-s_{1l_2}s_{4(-l_2)}s_{l_1l_2}$. For $m=3$ this construction determines the full cut, given by

$$\vcenter{\hbox{}}+\vcenter{\hbox{}}=-\frac{\mathrm{tr}(43l_121l_3)}{s_{2l_1}s_{3(-l_1)}s_{1l_3}s_{4(-l_3)}s_{l_1l_2}s_{l_2l_3}}\kappa\,.\qquad(6.7)$$

The trace arises as $\mathrm{tr}=\mathrm{tr}_++\mathrm{tr}_-$ from the two contributions.

6.1.2 MHV $\times$ MHV

The computation of two-particle cuts involving two MHV trees is analogous:

$$\vcenter{\hbox{}}=i\frac{\mathrm{tr}_+(l_1k(k+1)l_1l_2n1l_2)}{s_{1l_2}s_{kl_1}s_{(k+1)(-l_1)}s_{n(-l_2)}}A_n^{(0),\mathrm{MHV}}\,.\qquad(6.8)$$

When $k=2$ and $n=4$ we recover the two-particle cut (3.5) using $\mathrm{tr}_+(l_123l_1l_241l_2)=-sts_{3(-l_1)}s_{2l_1}$. The two MHV Parke-Taylor factors from the trees have been manipulated using

$$\frac{1}{\langle l_21\rangle\cdots\langle kl_1\rangle\langle l_1l_2\rangle}\times\frac{1}{\langle l_1(k+1)\rangle\cdots\langle nl_2\rangle\langle l_2l_1\rangle}$$
$$=-\underbrace{\frac{[l_1|k|k+1|l_1][l_2|n|1|l_2][l_1l_2]^2}{s_{1l_2}s_{kl_1}s_{(k+1)(-l_1)}s_{n(-l_2)}s_{l_1l_2}^2}}_{\text{phys. poles}}\underbrace{\frac{1}{\langle 12\rangle\cdots\langle n1\rangle}}_{\text{Parke-Taylor}}\,,\qquad(6.9)$$

and we inserted the supersum computed in (A.2) (with $\mathcal{N} = 4$ supersymmetries)

$$\int \mathrm{d}^{\mathcal{N}}\eta_{l_1}\mathrm{d}^{\mathcal{N}}\eta_{l_2}\delta^{2\mathcal{N}}(Q_{\mathrm{L}})\delta^{2\mathcal{N}}(Q_{\mathrm{R}}) = \langle l_1 l_2\rangle^{\mathcal{N}}\delta^{2\mathcal{N}}(Q)\,. \tag{6.10}$$

The cut with two $\overline{\mathrm{MHV}}$ trees is again given by replacing $|i\rangle \leftrightarrow |i]$.

6.2 $\mathcal{N} = 2$ SQCD

In $\mathcal{N} = 2$ SQCD there is a similar generalization, and we study cuts of the form

$$\begin{aligned}
&{}^{k}\underset{1}{\overset{l_1}{\text{\includegraphics}}}{}^{k+1}_{n} = \int \mathrm{d}^4\eta_{l_1}\cdots\mathrm{d}^4\eta_{l_m}\,A^{(0)}_{k+m,(ab)(cd)}(1,\ldots,k,l_1,\ldots,l_m)\\
&\hspace{5cm} A^{(0)}_{n-k+m,(ef)(gh)}(k+1,\ldots,n,-l_m,\ldots,-l_1)\,.
\end{aligned} \tag{6.11}$$

By analogy to $\kappa_{(ab)(cd)}$, we have introduced a new notation for tree amplitudes to encode the external-state configuration by projecting out external $\mathcal{N} = 2$ states from the $\mathcal{N} = 4$ Parke-Taylor formula (2.6):

$$A^{(0),\mathrm{MHV}}_{n,(ab)(cd)}(1,2,\ldots,n) = i\frac{\delta^4(Q)\eta_a^3\langle ab\rangle\eta_b^3\eta_c^4\langle cd\rangle\eta_d^4}{\langle 12\rangle\langle 23\rangle\cdots\langle n1\rangle}\,, \tag{6.12a}$$

$$A^{(0),\overline{\mathrm{MHV}}}_{n,(ab)(cd)}(1,2,\ldots,n) = i\frac{\delta^4(\bar{Q})\bar{\eta}_{a,3}[ab]\bar{\eta}_{b,3}\bar{\eta}_{c,4}[cd]\bar{\eta}_{d,4}}{[12][23]\cdots[n1]}\,, \tag{6.12b}$$

where in the former a, b, c, and d mark the legs carrying negative-helicity partons; in the latter these indices mark the positive-helicity partons. We study the same two possibilities as in $\mathcal{N} = 4$ SYM: $\overline{\mathrm{MHV}} \times \mathrm{MHV}$ and $\mathrm{MHV} \times \mathrm{MHV}$.

6.2.1 $\overline{\mathrm{MHV}} \times \mathrm{MHV}$

Once again specializing to $k = 2$ without loss of generality, we find the iterative structure of the cut as

$$\begin{aligned}
{}^{2}\underset{1}{\overset{l_1}{\text{\includegraphics}}}{}^{3}_{n} = \frac{i\,s_{12}\langle 2|3|l_1|2]\langle 1|l_m|n|1\rangle[ab][cd]\langle ef\rangle\langle gh\rangle[qr][st]}{s_{2l_1}s_{3(-l_1)}s_{1l_m}s_{n(-l_m)}s_{l_1l_2}\cdots s_{l_{r-1}l_r}}\frac{A^{(0),\mathrm{MHV}}_{n,(qr)(st)}}{s_{qr}s_{st}}\,.
\end{aligned} \tag{6.13}$$

To obtain this we have used the same superspace integral given earlier (6.4), this time with $\mathcal{N} = 2$ supersymmetries. By Lorentz invariance it is clear that the spinor-helicity objects always close to form Dirac traces; again, the opposite configuration is related by a CPT conjugation.

Further specializing to $r = 2$, the two-particle formula (3.19a) is recovered. For a final expression with $n = 4$ it is possible to cancel the unwanted s_{23} pole sitting in the tree-level factor and reintroduce $\kappa_{(qr)(st)}$:

$$\begin{aligned}
{}^{2}\underset{1}{\overset{l_1}{\text{\includegraphics}}}{}^{3}_{4} = -\frac{\langle 12\rangle\langle 1|l_m|4|3|l_1|2][ab][cd]\langle ef\rangle\langle gh\rangle[qr][st]}{s_{2l_1}s_{3(-l_1)}s_{1l_m}s_{4(-l_m)}s_{l_1l_2}\cdots s_{l_{m-1}l_m}s_{12}}\frac{\kappa_{(qr)(st)}}{s_{qr}s_{st}}\,.
\end{aligned} \tag{6.14}$$

These cuts do not introduce any new (unphysical) poles except the ones already found in the two-particle cut, which we identified as residues of the spinor-helicity notation (see section 3.2.3).

6.2.2 MHV × MHV

In this last example we obtain

$$
\begin{array}{c}
{}^{k}\!\!\!\underset{1}{\overset{l_1}{\longrightarrow}}\!\!\!\underset{l_2}{\overset{k+1}{\longrightarrow}}\!\!\!{}_{n}
\end{array}
= i\frac{[l_1|k|(k+1)|l_1][l_2|n|1|l_2]\langle ab\rangle\langle cd\rangle\langle ef\rangle\langle gh\rangle[qr][st]}{s_{1l_2}s_{kl_1}s_{(k+1)(-l_1)}s_{n(-l_2)}}\frac{A_{n,(qr)(st)}^{(0),\text{MHV}}}{s_{qr}s_{st}}\,,\quad (6.15)
$$

where the superspace integral (6.10) with $\mathcal{N}=2$ supersymmetries is used. Again, $\overline{\text{MHV}}\times\overline{\text{MHV}}$ is related by CPT conjugation.

7 Conclusions and outlook

In this paper we have developed an iterative method for calculating two-particle cuts in $\mathcal{N}=2$ SQCD — in essence, we have generalized the $\mathcal{N}=4$ SYM rung rule to $\mathcal{N}=2$ supersymmetries. The new technology allows us to write down expressions for all iterated two-particle cuts in four dimensions using simple diagrammatic rules. This eliminates the need for explicit state summation (Grassmann integration). Moreover, by factorizing physical propagators it expresses the cuts in a form that assigns contributions to individual diagrams and thus suggests their natural off-shell uplift. Armed with this new technology, we have found color-dual representations of all four-point massless $\mathcal{N}=2$ SQCD amplitudes up to two loops. We have also described extensions of the technology to multi-particle cuts.

The basic principle of the iteration is simple: when two tree amplitudes are glued together by summing over intermediate states, the result is always proportional to another tree amplitude. This means that the Grassmann integration can be performed once, and then re-used with each iteration. Propagators are exposed, so the expressions for contributing numerators can be lifted off shell, often without the need for ansätze. We expect this to work to all loop orders, inviting us to progress to three-loop $\mathcal{N}=2$ SQCD amplitudes.

We also expect the construction to work for lower-degree ($\mathcal{N}<2$) supersymmetry. The generalization of the supersum formula (3.12) to arbitrary $\mathcal{N}$ is discussed in ref. [122]. The remaining challenge is to eliminate the square root that appears, similarly to eq. (3.21), in the general formula. We anticipate that, while it may not be possible to find diagrammatic rules, such a construction will nevertheless make the propagator structure manifest. This should make it easier to lift expressions off shell, and we are encouraged to attempt two-loop $\mathcal{N}=0$ QCD examples.

With the ability to lift numerators directly from their cuts, we have seen hints of a close connection to the IR structure of the gauge theory. For instance, the one-loop box numerator with internal matter and external vectors, given in eq. (4.4), is completely IR regulated. Local integrands of this kind have already been studied by Badger, Peraro and one of the present authors [80, 119]. Similarly the one-loop mixed numerators vanish when loop momenta carried by internal hypermultiplets

become soft. In both cases, the appearance of Dirac traces naturally induce these properties.

The two-loop color-dual solution with four external vector multiplets, previously determined by Johansson and two of the present authors in ref. [66], also exhibits good IR structure. It contains chiral double-box numerators introduced by Caron-Huot and Larsen [120], which are IR finite when integrated to all orders in $\epsilon = (4-D)/2$. Their integrands are closely related to the chiral, BCFW-derived "local integrands" developed in planar $\mathcal{N}=4$ SYM, which also have good IR properties [4, 5, 7]. We also wonder whether such simplicity persists at three loops.

However, in other cases we encountered obstacles to finding simple color-dual integrands. We first noticed this in the one-loop solution with external matter multiplets — while a simple color-dual representation exists, it does not exhibit the IR properties we have come to expect. This persisted at two loops: in both cases with external matter, while we always found compact expressions for the cuts, extending them to off-shell color-dual numerators required more work. Nevertheless, knowing the terms appearing in different cuts allowed us to restrict our ansätze to certain terms, thus simplifying the computation.

Such obstacles are not uncommon in the pursuit of color-dual loop integrands. At three loops in $\mathcal{N}=4$ SYM, the rung rule does not give four-point color-dual numerators [4, 5, 59, 62, 102]; instead, it gives a representation matching the one in ref. [4]. Efforts to find a color-dual representation of the four-point, five-loop $\mathcal{N}=4$ integrand have faced similar impediments [11] — however, the need for such a representation to perform the double copy has now been circumvented to compute UV divergences in $\mathcal{N}=8$ supergravity [123–125]. Another conspicuous example is the five-gluon two-loop all-plus integrand: while non-local color-dual numerators were found requiring twelve powers of loop momentum [126], a planar local-integrand-based presentation is far more compact, with only four non-zero numerators [80, 119].

This suggests that our requirement of color-kinematics duality is, in some cases, creating tension between the off-shell numerators, so if our objective is not to use the double copy, we should consider relaxing it. Doing so would allow us to directly lift expressions for the numerators from their cuts; however, each numerator would then need to be computed separately. It would also be necessary to ensure that expressions for numerators coming from different cuts overlap with each other. The reward may be more chiral integrand structures for the two-loop solutions with external hypermultiplets.

A study of non-planar structures would also be required — we believe these can be isolated from iterated two-particle cuts. Local-integrand-like non-planar integrands have already been developed for $\mathcal{N}=4$ SYM [127]; the relevant integrals have logarithmic singularities manifested by expressing them in d*log* forms [12, 128]. In this paper, we have found examples of non-planar chiral integrands in the two-loop four-vector amplitude, which warrant further study.

We intend to explore these concepts further in an upcoming work, in which our main objective will be a better understanding of the interplay between local integrand representations and the IR structure of two-loop $\mathcal{N} = 2$ SQCD integrands.

Acknowledgments

A   Superspace calculus

In this section we detail the derivation of eqs. (6.10), (3.3) and (3.12). Grassmann variables are widely used in the literature to trivialize supersymmetric state sums, see notably refs. [121, 129]. Here we also restore some relative signs that we chose to omit in the main text.

We start by pointing out that already in eq. (2.7) there is a sign ambiguity due to an unspecified order of Grassmann multiplication inside $\delta^{2\mathcal{N}}(Q)$. We fix that sign by taking the right-hand side of eq. (2.7) as the definition of the Grassmann delta function. Then we can use the Schouten identity to derive the following identity valid for any p and q such that $\langle pq \rangle \neq 0$:

$$\delta^{2\mathcal{N}}\left(\sum_{i=1}^{n} |i\rangle \eta_i \right) \equiv \prod_{I=1}^{\mathcal{N}} \sum_{i<j}^{n} \langle i\,j \rangle \eta_i^I \eta_j^I = \frac{1}{\langle pq \rangle^{\mathcal{N}}} \, \delta^{\mathcal{N}}\left(\sum_{i=1}^{n} \langle pi \rangle \eta_i \right) \delta^{\mathcal{N}}\left(\sum_{i=1}^{n} \langle qi \rangle \eta_i \right). \quad \text{(A.1)}$$

Using this identity twice, we compute the supersum (6.10) relevant for a general

two-particle MHV × MHV:

$$\int \mathrm{d}^{\mathcal{N}}\eta_{l_1}\mathrm{d}^{\mathcal{N}}\eta_{l_2}\delta^{2\mathcal{N}}(Q_{\mathrm{L}})\delta^{2\mathcal{N}}(Q_{\mathrm{R}}) \tag{A.2}$$

$$= \int \mathrm{d}^{\mathcal{N}}\eta_{l_1}\mathrm{d}^{\mathcal{N}}\eta_{l_2}\delta^{2\mathcal{N}}\!\left(|l_1\rangle\eta_{l_1} + |l_2\rangle\eta_{l_2} + \sum_{i=1}^{k}|i\rangle\eta_i\right)\delta^{2\mathcal{N}}\!\left(-|l_1\rangle\eta_{l_1} - |l_2\rangle\eta_{l_2} + \sum_{i=k+1}^{n}|i\rangle\eta_i\right)$$

$$= \frac{1}{\langle l_1 l_2\rangle^{2\mathcal{N}}}\int \mathrm{d}^{\mathcal{N}}\eta_{l_1}\mathrm{d}^{\mathcal{N}}\eta_{l_2}\delta^{\mathcal{N}}\!\left(\langle l_1 l_2\rangle\eta_{l_2} + \sum_{i=1}^{k}\langle l_1 i\rangle\eta_i\right)\delta^{\mathcal{N}}\!\left(\langle l_2 l_1\rangle\eta_{l_1} + \sum_{i=1}^{k}\langle l_2 i\rangle\eta_i\right)$$

$$\times\, \delta^{\mathcal{N}}\!\left(\langle l_1 l_2\rangle\eta_{l_2} - \sum_{i=k+1}^{n}\langle l_1 i\rangle\eta_i\right)\delta^{\mathcal{N}}\!\left(\langle l_2 l_1\rangle\eta_{l_1} - \sum_{i=k+1}^{n}\langle l_2 i\rangle\eta_i\right)$$

$$= \delta^{\mathcal{N}}\!\left(\sum_{i=1}^{n}\langle l_1 i\rangle\eta_i\right)\delta^{\mathcal{N}}\!\left(\sum_{i=1}^{n}\langle l_2 i\rangle\eta_i\right) = \langle l_1 l_2\rangle^{\mathcal{N}}\delta^{2\mathcal{N}}(Q)\,.$$

It is now effortless to verify the $\mathcal{N} = 4$ supersum in eq. (3.3):

$$\int \mathrm{d}^4\eta_{l_1}\mathrm{d}^4\eta_{l_2}\kappa(1,2,l_1,l_2)\kappa(3,4,-l_2,-l_1) = \frac{[12][34][l_1 l_2]^2}{\langle 12\rangle\langle 34\rangle\langle l_1 l_2\rangle^2}\int \mathrm{d}^4\eta_{l_1}\mathrm{d}^4\eta_{l_2}\delta^8(Q_{\mathrm{L}})\delta^8(Q_{\mathrm{R}})$$

$$= \frac{[12][34]\langle l_1 l_2\rangle^2[l_1 l_2]^2}{\langle 12\rangle\langle 34\rangle}\delta^8\!\left(\sum_{i=1}^{4}|i\rangle\eta_i\right) = s_{l_1 l_2}^2\,\kappa(1,2,3,4)\,. \tag{A.3}$$

The $\mathcal{N} = 2$ supersum in eq. (3.12) is handled similarly

$$\int \mathrm{d}^4\eta_{l_1}\mathrm{d}^4\eta_{l_2}\kappa_{(ab)(cd)}(1,2,l_1,l_2)\kappa_{(ef)(gh)}(3,4,-l_2,-l_1)$$

$$= \frac{[12][34][l_1 l_2]^2}{\langle 12\rangle\langle 34\rangle\langle l_1 l_2\rangle^2}\int \mathrm{d}^4\eta_{l_1}\mathrm{d}^4\eta_{l_2}\delta^4(Q_{\mathrm{L}})\langle ab\rangle\langle cd\rangle\eta_a^3\eta_b^3\eta_c^4\eta_d^4 \times \delta^4(Q_{\mathrm{R}})\langle ef\rangle\langle gh\rangle\eta_e^3\eta_f^3\eta_g^4\eta_h^4$$

$$= \frac{[12][34][l_1 l_2]^2}{\langle 12\rangle\langle 34\rangle\langle l_1 l_2\rangle^2}\int \mathrm{d}^2\eta_{l_1}\mathrm{d}^2\eta_{l_2}\delta^4(Q_{\mathrm{L}})\delta^4(Q_{\mathrm{R}}) \tag{A.4}$$

$$\times\int \mathrm{d}\eta_{l_1}^4\mathrm{d}\eta_{l_1}^3\mathrm{d}\eta_{l_2}^4\mathrm{d}\eta_{l_2}^3\,(\eta_a^3\eta_b^3\eta_c^4\eta_d^4)(\eta_e^3\eta_f^3\eta_g^4\eta_h^4)\langle ab\rangle\langle cd\rangle\langle ef\rangle\langle gh\rangle$$

$$= \frac{[12][34][l_1 l_2]^2}{\langle 12\rangle\langle 34\rangle}\delta^4(Q)\int \mathrm{d}\eta_{l_1}^4\mathrm{d}\eta_{l_1}^3\mathrm{d}\eta_{l_2}^4\mathrm{d}\eta_{l_2}^3\,(\eta_a^3\eta_b^3\eta_c^4\eta_d^4)(\eta_e^3\eta_f^3\eta_g^4\eta_h^4)\langle ab\rangle\langle cd\rangle\langle ef\rangle\langle gh\rangle$$

$$= \mathrm{sgn}(abcd)\,\mathrm{sgn}(efgh)[l_1 l_2]^2\langle ab\rangle\langle cd\rangle\langle ef\rangle\langle gh\rangle[qr][st]\frac{\kappa_{(qr)(st)}}{s_{qr}s_{st}}\,,$$

up to the last step in the derivation, where we have used the fact that the broken-superspace variables must factorize onto the external ones comprising $\kappa_{(qr)(st)}$ and the internal ones annihilated by the remaining Grassmann integration,

$$(\eta_a^3\eta_b^3\eta_c^4\eta_d^4)(\eta_e^3\eta_f^3\eta_g^4\eta_h^4) = (\eta_{l_1}^3\eta_{l_1}^4\eta_{l_2}^3\eta_{l_2}^4)(\eta_q^3\eta_r^3\eta_s^4\eta_t^4)\,. \tag{A.5}$$

The signs $\mathrm{sgn}(abcd)$ and $\mathrm{sgn}(efgh)$ are determined by the permutation signatures with respect to $\{q,r,l_1,l_2\}$ and $\{s,t,l_1,l_2\}$, respectively.

	Two-term id.	Manifest CPT	Matter reversal	$\mathcal{N} = 4$
1-loop vectors	✓	✓	✓	✓
1-loop mixed	✓	✓	✓	✓
1-loop matter	✓	✓	✓	✓
1-loop matter alt.	✓	✓	$\times^*$	$\times$
2-loop vectors	✓	✓	✓	✓
2-loop mixed	✓	✓	✓	✓
2-loop matter	✓	✓	$\times^*$	$\times$

Table 2: Properties of the various solutions summarized: two-term identities (see section 2.3.1), manifest CPT invariance (see section 2.3.2), matter-reversal symmetry (see section 2.3.3), and adding up to $\mathcal{N} = 4$ (see section 2.3.4). *Matter-reversal symmetry works for all numerators except for some of those with matter tadpoles. The symmetry can still be used to reduce the set of masters for all other topologies.

B All integrands summarized

In this section we summarize the full color-dual representation of all one- and two-loop integrands for $\mathcal{N} = 2$ SQCD. The one-loop results are short enough to be explicitly written out here. The two-loop integrands are quite lengthy, but they, as well as their one-loop counterpart, can be downloaded as ancillary files. Table 2 summarizes which representations fulfill the properties discussed in section 2.3.

All representations are attached in a machine-readable format to the arXiv submission of this paper. The ancillary files for each solution are named:

- One-loop external vectors: `ancillaryLeq1Vectors.m`

- One-loop mixed: `ancillaryLeq1Mixed.m`

- One-loop external matter: `ancillaryLeq1Matter.m`

- Two-loop external vectors: `ancillaryLeq2Vectors.m`

- Two-loop mixed: `ancillaryLeq2Mixed.m`

- Two-loop external matter: `ancillaryLeq2Matter.m`

The files are optimized for usage with Mathematica, but the format is general enough to allow for an import into any other computer algebra system. Each file contains a short overview of its contents in the start.

B.1 One-loop external vectors

$$n\left(\text{}\right) = \hat{\kappa}_{13}\,\text{tr}_-(1(\ell - p_1)(\ell + p_4)3) + \hat{\kappa}_{24}\,\text{tr}_+(1(\ell - p_1)(\ell + p_4)3) \qquad \text{(B.1a)}$$
$$+\mu^2\big(s(\hat{\kappa}_{12}+\hat{\kappa}_{34}) + t(\hat{\kappa}_{23}+\hat{\kappa}_{14}) + u(\hat{\kappa}_{13}+\hat{\kappa}_{24})\big)\,,$$

$$n\left(\text{}\right) = (\hat{\kappa}_{13} + \hat{\kappa}_{34})\,\text{tr}_-(1(\ell - p_1)(\ell + p_4)3) \qquad \text{(B.1b)}$$
$$+ (\hat{\kappa}_{12} + \hat{\kappa}_{24})\,\text{tr}_+(1(\ell - p_1)(\ell + p_4)3) + (\hat{\kappa}_{12} + \hat{\kappa}_{34})t\ell^2\,,$$

$$n\left(\text{}\right) = 2\ell\cdot(p_{12} - \ell)\big[t(\hat{\kappa}_{23} + \hat{\kappa}_{14}) - u(\hat{\kappa}_{13} + \hat{\kappa}_{24})\big]\,, \qquad \text{(B.1c)}$$

$$n\left(\text{}\right) = 2\ell\cdot(p_4 + \ell)\big[u(\hat{\kappa}_{13} + \hat{\kappa}_{24}) - t(\hat{\kappa}_{14} + \hat{\kappa}_{23})\big]\,, \qquad \text{(B.1d)}$$

$$n\left(\text{}\right) = 4(\ell \cdot p_4)\big[u(\hat{\kappa}_{13} + \hat{\kappa}_{24}) - t(\hat{\kappa}_{14} + \hat{\kappa}_{23})\big]\,, \qquad \text{(B.1e)}$$

$$n\left(\text{}\right) = 4(\ell \cdot p_{34})\big[u(\hat{\kappa}_{13} + \hat{\kappa}_{24}) - t(\hat{\kappa}_{14} + \hat{\kappa}_{23})\big]\,, \qquad \text{(B.1f)}$$

$$n\left(\text{}\right) = n^{[\mathcal{N}=4]}\left(\text{}\right) - 2n\left(\text{}\right)\,, \qquad \text{(B.1g)}$$

$$n\left(\text{}\right) = -2n\left(\text{}\right)\,, \qquad \text{(B.1h)}$$

$$n\left(\text{}\right) = -2n\left(\text{}\right)\,, \quad n\left(\text{}\right) = -2n\left(\text{}\right)\,, \qquad \text{(B.1i)}$$

$$n\left(\text{}\right) = -2n\left(\text{}\right)\,, \qquad n\left(\text{}\right) = -2n\left(\text{}\right)\,. \qquad \text{(B.1j)}$$

B.2 One-loop external vectors + matter

$$n\left(\text{}\right) = \hat{\kappa}_{(12)(13)}\,\text{tr}_+(4\ell12) + \hat{\kappa}_{(24)(34)}\,\text{tr}_-(4\ell12)\,, \qquad \text{(B.2a)}$$

$$n\left(\text{}\right) = \hat{\kappa}_{(12)(14)}\,\text{tr}_+(3\ell12) + \hat{\kappa}_{(23)(34)}\,\text{tr}_-(3\ell12)\,, \qquad \text{(B.2b)}$$

$$n\left(\text{}\right) = \hat{\kappa}_{(12)(24)}\,\text{tr}_+(3\ell21) + \hat{\kappa}_{(13)(34)}\,\text{tr}_-(3\ell21)\,, \qquad \text{(B.2c)}$$

$$n\left(\text{}\right) = -\frac{1}{2}n\left(\text{}\right) = \hat{\kappa}_{(12)(13)}\,\text{tr}_+(4\ell12) + \hat{\kappa}_{(24)(34)}\,\text{tr}_-(4\ell12)\,. \qquad \text{(B.2d)}$$

– 38 –

B.3 One-loop external matter

$$n\left(\text{[diagram]}\right) = -su\,\hat{\kappa}_{(13)(24)}\,, \qquad n\left(\text{[diagram]}\right) = s^2\,\hat{\kappa}_{(12)(34)}\,, \quad \text{(B.3a)}$$

$$n\left(\text{[diagram]}\right) = -n\left(\text{[diagram]}\right) = -su\,\hat{\kappa}_{(13)(24)}\,, \qquad\qquad \text{(B.3b)}$$

$$n\left(\text{[diagram]}\right) = -\frac{1}{2}n\left(\text{[diagram]}\right) = -su\,\hat{\kappa}_{(13)(24)}\,. \qquad\qquad \text{(B.3c)}$$

References

[1] S. Caron-Huot, L. J. Dixon, A. McLeod and M. von Hippel, *Bootstrapping a Five-Loop Amplitude Using Steinmann Relations*, *Phys. Rev. Lett.* **117** (2016) 241601 [1609.00669].

[2] C. Anastasiou, Z. Bern, L. J. Dixon and D. A. Kosower, *Planar amplitudes in maximally supersymmetric Yang-Mills theory*, *Phys. Rev. Lett.* **91** (2003) 251602 [hep-th/0309040].

[3] Z. Bern, L. J. Dixon and V. A. Smirnov, *Iteration of planar amplitudes in maximally supersymmetric Yang-Mills theory at three loops and beyond*, *Phys. Rev.* **D72** (2005) 085001 [hep-th/0505205].

[4] N. Arkani-Hamed, J. L. Bourjaily, F. Cachazo, S. Caron-Huot and J. Trnka, *The All-Loop Integrand For Scattering Amplitudes in Planar N=4 SYM*, *JHEP* **1101** (2011) 041 [1008.2958].

[5] N. Arkani-Hamed, J. L. Bourjaily, F. Cachazo and J. Trnka, *Local Integrals for Planar Scattering Amplitudes*, *JHEP* **06** (2012) 125 [1012.6032].

[6] N. Arkani-Hamed, J. L. Bourjaily, F. Cachazo, A. B. Goncharov, A. Postnikov and J. Trnka, *Grassmannian Geometry of Scattering Amplitudes*. Cambridge University Press, 2016, 10.1017/CBO9781316091548, [1212.5605].

[7] J. L. Bourjaily and J. Trnka, *Local Integrand Representations of All Two-Loop Amplitudes in Planar SYM*, *JHEP* **08** (2015) 119 [1505.05886].

[8] Z. Bern, J. Carrasco, L. J. Dixon, H. Johansson, D. Kosower et al., *Three-Loop Superfiniteness of N=8 Supergravity*, *Phys.Rev.Lett.* **98** (2007) 161303 [hep-th/0702112].

[9] Z. Bern, J. Carrasco, L. J. Dixon, H. Johansson and R. Roiban, *The Complete Four-Loop Four-Point Amplitude in N=4 Super-Yang-Mills Theory*, *Phys.Rev.* **D82** (2010) 125040 [1008.3327].

[10] J. J. M. Carrasco and H. Johansson, *Five-Point Amplitudes in N=4 Super-Yang-Mills Theory and N=8 Supergravity*, *Phys.Rev.* **D85** (2012) 025006 [1106.4711].

[11] Z. Bern, J. Carrasco, H. Johansson and R. Roiban, *The Five-Loop Four-Point Amplitude of N=4 super-Yang-Mills Theory*, *Phys.Rev.Lett.* **109** (2012) 241602 [`1207.6666`].

[12] Z. Bern, E. Herrmann, S. Litsey, J. Stankowicz and J. Trnka, *Evidence for a Nonplanar Amplituhedron*, *JHEP* **06** (2016) 098 [`1512.08591`].

[13] J. M. Henn and B. Mistlberger, *Four-Gluon Scattering at Three Loops, Infrared Structure, and the Regge Limit*, *Phys. Rev. Lett.* **117** (2016) 171601 [`1608.00850`].

[14] C. Anastasiou, E. W. N. Glover, C. Oleari and M. E. Tejeda-Yeomans, *Two-loop QCD corrections to the scattering of massless distinct quarks*, *Nucl. Phys.* **B601** (2001) 318 [`hep-ph/0010212`].

[15] C. Anastasiou, E. W. N. Glover, C. Oleari and M. E. Tejeda-Yeomans, *Two loop QCD corrections to massless identical quark scattering*, *Nucl. Phys.* **B601** (2001) 341 [`hep-ph/0011094`].

[16] C. Anastasiou, E. W. N. Glover, C. Oleari and M. E. Tejeda-Yeomans, *Two loop QCD corrections to massless quark gluon scattering*, *Nucl. Phys.* **B605** (2001) 486 [`hep-ph/0101304`].

[17] E. W. N. Glover, C. Oleari and M. E. Tejeda-Yeomans, *Two loop QCD corrections to gluon-gluon scattering*, *Nucl. Phys.* **B605** (2001) 467 [`hep-ph/0102201`].

[18] L. W. Garland, T. Gehrmann, E. W. N. Glover, A. Koukoutsakis and E. Remiddi, *The Two loop QCD matrix element for e+ e- → 3 jets*, *Nucl. Phys.* **B627** (2002) 107 [`hep-ph/0112081`].

[19] L. W. Garland, T. Gehrmann, E. W. N. Glover, A. Koukoutsakis and E. Remiddi, *Two loop QCD helicity amplitudes for e+ e- → three jets*, *Nucl. Phys.* **B642** (2002) 227 [`hep-ph/0206067`].

[20] S. Catani, L. Cieri, D. de Florian, G. Ferrera and M. Grazzini, *Diphoton production at hadron colliders: a fully-differential QCD calculation at NNLO*, *Phys. Rev. Lett.* **108** (2012) 072001 [`1110.2375`].

[21] T. Gehrmann, M. Jaquier, E. Glover and A. Koukoutsakis, *Two-Loop QCD Corrections to the Helicity Amplitudes for H → 3 partons*, *JHEP* **1202** (2012) 056 [`1112.3554`].

[22] M. Czakon, P. Fiedler and A. Mitov, *Total Top-Quark Pair-Production Cross Section at Hadron Colliders Through $O(\alpha_S^4)$*, *Phys.Rev.Lett.* **110** (2013) 252004 [`1303.6254`].

[23] M. Grazzini, S. Kallweit, D. Rathlev and A. Torre, *$Z\gamma$ production at hadron colliders in NNLO QCD*, *Phys.Lett.* **B731** (2014) 204 [`1309.7000`].

[24] F. Cascioli, T. Gehrmann, M. Grazzini, S. Kallweit, P. Maierhöfer et al., *ZZ production at hadron colliders in NNLO QCD*, *Phys.Lett.* **B735** (2014) 311 [`1405.2219`].

[25] T. Gehrmann, M. Grazzini, S. Kallweit, P. Maierhöfer, A. von Manteuffel et al., *W$^+$W$^-$ Production at Hadron Colliders in Next to Next to Leading Order QCD*, *Phys.Rev.Lett.* **113** (2014) 212001 [1408.5243].

[26] X. Chen, T. Gehrmann, E. Glover and M. Jaquier, *Precise QCD predictions for the production of Higgs + jet final states*, *Phys.Lett.* **B740** (2015) 147 [1408.5325].

[27] F. Caola, J. M. Henn, K. Melnikov, A. V. Smirnov and V. A. Smirnov, *Two-loop helicity amplitudes for the production of two off-shell electroweak bosons in quark-antiquark collisions*, *JHEP* **1411** (2014) 041 [1408.6409].

[28] M. Czakon, P. Fiedler and A. Mitov, *Resolving the Tevatron Top Quark Forward-Backward Asymmetry Puzzle: Fully Differential Next-to-Next-to-Leading-Order Calculation*, *Phys. Rev. Lett.* **115** (2015) 052001 [1411.3007].

[29] T. Gehrmann, A. von Manteuffel and L. Tancredi, *The two-loop helicity amplitudes for $q\bar{q}' \to V_1V_2 \to 4$ leptons*, *JHEP* **09** (2015) 128 [1503.04812].

[30] F. Caola, J. M. Henn, K. Melnikov, A. V. Smirnov and V. A. Smirnov, *Two-loop helicity amplitudes for the production of two off-shell electroweak bosons in gluon fusion*, *JHEP* **1506** (2015) 129 [1503.08759].

[31] A. von Manteuffel and L. Tancredi, *The two-loop helicity amplitudes for $gg \to V_1V_2 \to 4$ leptons*, *JHEP* **1506** (2015) 197 [1503.08835].

[32] M. Grazzini, S. Kallweit and D. Rathlev, *$W\gamma$ and $Z\gamma$ production at the LHC in NNLO QCD*, *JHEP* **07** (2015) 085 [1504.01330].

[33] R. Boughezal, C. Focke, X. Liu and F. Petriello, *W-boson production in association with a jet at next-to-next-to-leading order in perturbative QCD*, *Phys. Rev. Lett.* **115** (2015) 062002 [1504.02131].

[34] R. Boughezal, F. Caola, K. Melnikov, F. Petriello and M. Schulze, *Higgs boson production in association with a jet at next-to-next-to-leading order*, *Phys. Rev. Lett.* **115** (2015) 082003 [1504.07922].

[35] R. Boughezal, C. Focke, W. Giele, X. Liu and F. Petriello, *Higgs boson production in association with a jet using jettiness subtraction*, *Phys.Lett.* **B748** (2015) 5 [1505.03893].

[36] A. Gehrmann-De Ridder, T. Gehrmann, E. W. N. Glover, A. Huss and T. A. Morgan, *Precise QCD predictions for the production of a Z boson in association with a hadronic jet*, *Phys. Rev. Lett.* **117** (2016) 022001 [1507.02850].

[37] C. Anastasiou, C. Duhr, F. Dulat, F. Herzog and B. Mistlberger, *Higgs Boson Gluon-Fusion Production in QCD at Three Loops*, *Phys.Rev.Lett.* **114** (2015) 212001 [1503.06056].

[38] Z. Bern, L. J. Dixon, D. C. Dunbar and D. A. Kosower, *One-Loop n-Point Gauge Theory Amplitudes, Unitarity and Collinear Limits*, *Nucl. Phys.* **B425** (1994) 217 [hep-ph/9403226].

[39] Z. Bern, L. J. Dixon, D. C. Dunbar and D. A. Kosower, *Fusing gauge theory tree amplitudes into loop amplitudes*, *Nucl.Phys.* **B435** (1995) 59 [hep-ph/9409265].

[40] R. Britto, F. Cachazo and B. Feng, *Generalized unitarity and one-loop amplitudes in N=4 super-Yang-Mills*, *Nucl.Phys.* **B725** (2005) 275 [hep-th/0412103].

[41] R. Britto, F. Cachazo and B. Feng, *New recursion relations for tree amplitudes of gluons*, *Nucl.Phys.* **B715** (2005) 499 [hep-th/0412308].

[42] R. Britto, F. Cachazo, B. Feng and E. Witten, *Direct proof of tree-level recursion relation in Yang-Mills theory*, *Phys.Rev.Lett.* **94** (2005) 181602 [hep-th/0501052].

[43] D. Forde, *Direct extraction of one-loop integral coefficients*, *Phys.Rev.* **D75** (2007) 125019 [0704.1835].

[44] C. Anastasiou, R. Britto, B. Feng, Z. Kunszt and P. Mastrolia, *D-dimensional unitarity cut method*, *Phys. Lett.* **B645** (2007) 213 [hep-ph/0609191].

[45] W. T. Giele, Z. Kunszt and K. Melnikov, *Full one-loop amplitudes from tree amplitudes*, *JHEP* **0804** (2008) 049 [0801.2237].

[46] S. Badger, H. Frellesvig and Y. Zhang, *A Two-Loop Five-Gluon Helicity Amplitude in QCD*, *JHEP* **1312** (2013) 045 [1310.1051].

[47] S. Badger, G. Mogull, A. Ochirov and D. O'Connell, *A Complete Two-Loop, Five-Gluon Helicity Amplitude in Yang-Mills Theory*, *JHEP* **10** (2015) 064 [1507.08797].

[48] T. Gehrmann, J. M. Henn and N. A. Lo Presti, *Analytic form of the two-loop planar five-gluon all-plus-helicity amplitude in QCD*, *Phys. Rev. Lett.* **116** (2016) 062001 [1511.05409].

[49] S. Badger, C. Bronnum-Hansen, H. B. Hartanto and T. Peraro, *First look at two-loop five-gluon scattering in QCD*, *Phys. Rev. Lett.* **120** (2018) 092001 [1712.02229].

[50] S. Abreu, F. Febres Cordero, H. Ita, B. Page and M. Zeng, *Planar Two-Loop Five-Gluon Amplitudes from Numerical Unitarity*, *Phys. Rev.* **D97** (2018) 116014 [1712.03946].

[51] H. A. Chawdhry, M. A. Lim and A. Mitov, *Two-loop five-point massless QCD amplitudes within the IBP approach*, 1805.09182.

[52] S. Badger, C. Bronnum-Hansen, T. Gehrmann, H. B. Hartanto, J. Henn, N. A. Lo Presti et al., *Applications of integrand reduction to two-loop five-point scattering amplitudes in QCD*, *PoS* **LL2018** (2018) 006 [1807.09709].

[53] S. Abreu, F. Febres Cordero, H. Ita, B. Page and V. Sotnikov, *Planar Two-Loop Five-Parton Amplitudes from Numerical Unitarity*, 1809.09067.

[54] L. J. Dixon, *Calculating scattering amplitudes efficiently*, in *QCD and beyond. Proceedings, Theoretical Advanced Study Institute in Elementary Particle Physics, TASI-95, Boulder, USA, June 4-30, 1995*, pp. 539–584, 1996, hep-ph/9601359,

http://www-public.slac.stanford.edu/sciDoc/docMeta.aspx?slacPubNumber=SLAC-PUB-7106.

[55] L. J. Dixon, J. M. Henn, J. Plefka and T. Schuster, *All tree-level amplitudes in massless QCD*, *JHEP* **1101** (2011) 035 [`1010.3991`].

[56] T. Melia, *Getting more flavor out of one-flavor QCD*, *Phys.Rev.* **D89** (2014) 074012 [`1312.0599`].

[57] Z. Bern, L. J. Dixon and D. A. Kosower, *One loop corrections to five gluon amplitudes*, *Phys.Rev.Lett.* **70** (1993) 2677 [`hep-ph/9302280`].

[58] Z. Bern, A. De Freitas, L. J. Dixon and H. L. Wong, *Supersymmetric regularization, two loop QCD amplitudes and coupling shifts*, *Phys. Rev.* **D66** (2002) 085002 [`hep-ph/0202271`].

[59] Z. Bern, J. S. Rozowsky and B. Yan, *Two loop four gluon amplitudes in N=4 superYang-Mills*, *Phys. Lett.* **B401** (1997) 273 [`hep-ph/9702424`].

[60] Z. Bern, L. J. Dixon, D. C. Dunbar, M. Perelstein and J. S. Rozowsky, *On the relationship between Yang-Mills theory and gravity and its implication for ultraviolet divergences*, *Nucl. Phys.* **B530** (1998) 401 [`hep-th/9802162`].

[61] Z. Bern, J. Carrasco and H. Johansson, *New Relations for Gauge-Theory Amplitudes*, *Phys.Rev.* **D78** (2008) 085011 [`0805.3993`].

[62] Z. Bern, J. J. M. Carrasco and H. Johansson, *Perturbative Quantum Gravity as a Double Copy of Gauge Theory*, *Phys.Rev.Lett.* **105** (2010) 061602 [`1004.0476`].

[63] H. Johansson and A. Ochirov, *Color-Kinematics Duality for QCD Amplitudes*, *JHEP* **01** (2016) 170 [`1507.00332`].

[64] M. Chiodaroli, Q. Jin and R. Roiban, *Color/kinematics duality for general abelian orbifolds of N=4 super Yang-Mills theory*, *JHEP* **1401** (2014) 152 [`1311.3600`].

[65] H. Johansson and A. Ochirov, *Pure Gravities via Color-Kinematics Duality for Fundamental Matter*, *JHEP* **11** (2015) 046 [`1407.4772`].

[66] H. Johansson, G. Kälin and G. Mogull, *Two-loop supersymmetric QCD and half-maximal supergravity amplitudes*, *JHEP* **09** (2017) 019 [`1706.09381`].

[67] Z. Bern, C. Boucher-Veronneau and H. Johansson, *N ≥ 4 Supergravity Amplitudes from Gauge Theory at One Loop*, *Phys.Rev.* **D84** (2011) 105035 [`1107.1935`].

[68] J. J. M. Carrasco, M. Chiodaroli, M. Gunaydin and R. Roiban, *One-loop four-point amplitudes in pure and matter-coupled $\mathcal{N} \leq 4$ supergravity*, *JHEP* **1303** (2013) 056 [`1212.1146`].

[69] M. Chiodaroli, M. Günaydin, H. Johansson and R. Roiban, *Scattering amplitudes in $\mathcal{N} = 2$ Maxwell-Einstein and Yang-Mills/Einstein supergravity*, *JHEP* **1501** (2015) 081 [`1408.0764`].

[70] M. Chiodaroli, M. Gunaydin, H. Johansson and R. Roiban, *Spontaneously Broken*

Yang-Mills-Einstein Supergravities as Double Copies, *JHEP* **06** (2017) 064 [1511.01740].

[71] M. Chiodaroli, M. Gunaydin, H. Johansson and R. Roiban, *Complete construction of magical, symmetric and homogeneous N=2 supergravities as double copies of gauge theories*, *Phys. Rev. Lett.* **117** (2016) 011603 [1512.09130].

[72] A. Anastasiou, L. Borsten, M. J. Duff, M. J. Hughes, A. Marrani, S. Nagy et al., *Twin supergravities from Yang-Mills theory squared*, *Phys. Rev.* **D96** (2017) 026013 [1610.07192].

[73] H. Johansson and J. Nohle, *Conformal Gravity from Gauge Theory*, 1707.02965.

[74] M. Chiodaroli, M. Gunaydin, H. Johansson and R. Roiban, *Gauged Supergravities and Spontaneous Supersymmetry Breaking from the Double Copy Construction*, *Phys. Rev. Lett.* **120** (2018) 171601 [1710.08796].

[75] H. Johansson, G. Mogull and F. Teng, *Unraveling conformal gravity amplitudes*, *JHEP* **09** (2018) 080 [1806.05124].

[76] E. W. N. Glover, V. V. Khoze and C. Williams, *Component MHV amplitudes in N=2 SQCD and in N=4 SYM at one loop*, *JHEP* **08** (2008) 033 [0805.4190].

[77] R. Andree and D. Young, *Wilson Loops in N=2 Superconformal Yang-Mills Theory*, *JHEP* **09** (2010) 095 [1007.4923].

[78] M. Leoni, A. Mauri and A. Santambrogio, *Four-point amplitudes in $\mathcal{N} = 2$ SCQCD*, *JHEP* **09** (2014) 017 [1406.7283].

[79] M. Leoni, A. Mauri and A. Santambrogio, *On the amplitude/Wilson loop duality in N=2 SCQCD*, *Phys. Lett.* **B747** (2015) 325 [1502.07614].

[80] S. Badger, G. Mogull and T. Peraro, *Local integrands for two-loop all-plus Yang-Mills amplitudes*, *JHEP* **08** (2016) 063 [1606.02244].

[81] Z. Bern, L. J. Dixon and D. Kosower, *A Two loop four gluon helicity amplitude in QCD*, *JHEP* **0001** (2000) 027 [hep-ph/0001001].

[82] D. C. Dunbar and W. B. Perkins, *Two-loop five-point all plus helicity Yang-Mills amplitude*, *Phys. Rev.* **D93** (2016) 085029 [1603.07514].

[83] D. C. Dunbar, G. R. Jehu and W. B. Perkins, *The two-loop n-point all-plus helicity amplitude*, *Phys. Rev.* **D93** (2016) 125006 [1604.06631].

[84] D. C. Dunbar, G. R. Jehu and W. B. Perkins, *Two-loop six gluon all plus helicity amplitude*, *Phys. Rev. Lett.* **117** (2016) 061602 [1605.06351].

[85] Z. Bern, L. J. Dixon, D. C. Dunbar and D. A. Kosower, *One loop selfdual and N=4 super Yang-Mills*, *Phys.Lett.* **B394** (1997) 105 [hep-th/9611127].

[86] V. Nair, *A Current Algebra for Some Gauge Theory Amplitudes*, *Phys.Lett.* **B214** (1988) 215.

[87] N. Bjerrum-Bohr, D. C. Dunbar and W. B. Perkins, *Analytic structure of three-mass triangle coefficients*, *JHEP* **0804** (2008) 038 [0709.2086].

[88] A. Ochirov, *All one-loop NMHV gluon amplitudes in N=1 SYM*, *JHEP* **12** (2013) 080 [`1311.1491`].

[89] S. J. Parke and T. Taylor, *An Amplitude for n Gluon Scattering*, *Phys.Rev.Lett.* **56** (1986) 2459.

[90] H. Elvang and Y.-t. Huang, *Scattering Amplitudes in Gauge Theory and Gravity*. Cambridge University Press, 2015.

[91] A. Ochirov and B. Page, *Full Colour for Loop Amplitudes in Yang-Mills Theory*, *JHEP* **02** (2017) 100 [`1612.04366`].

[92] G. Kälin, *Cyclic Mario worlds — color-decomposition for one-loop QCD*, *JHEP* **04** (2018) 141 [`1712.03539`].

[93] M. Kiermaier, *Gravity as the square of gauge theory*, talk at conference Amplitudes, 2010, http://strings.ph.qmul.ac.uk/ theory/Amplitudes2010/Talks/MK2010.pdf.

[94] N. Bjerrum-Bohr, P. H. Damgaard, T. Sondergaard and P. Vanhove, *The Momentum Kernel of Gauge and Gravity Theories*, *JHEP* **1101** (2011) 001 [`1010.3933`].

[95] N. Bjerrum-Bohr, P. H. Damgaard and P. Vanhove, *Minimal Basis for Gauge Theory Amplitudes*, *Phys.Rev.Lett.* **103** (2009) 161602 [`0907.1425`].

[96] S. Stieberger, *Open & Closed vs. Pure Open String Disk Amplitudes*, `0907.2211`.

[97] B. Feng, R. Huang and Y. Jia, *Gauge Amplitude Identities by On-shell Recursion Relation in S-matrix Program*, *Phys.Lett.* **B695** (2011) 350 [`1004.3417`].

[98] L. de la Cruz, A. Kniss and S. Weinzierl, *Proof of the fundamental BCJ relations for QCD amplitudes*, *JHEP* **09** (2015) 197 [`1508.01432`].

[99] M. Chiodaroli, *Simplifying amplitudes in Maxwell-Einstein and Yang-Mills-Einstein supergravities*, in *Jochen Brüning, Matthias Staudacher (Eds.), Space – Time – Matter: Analytic and Geometric Structures. Berlin, Boston: De Gruyter.*, pp. 266–287, 2018, `1607.04129`, DOI.

[100] Z. Bern, L. J. Dixon and D. A. Kosower, *N=4 super-Yang-Mills theory, QCD and collider physics*, *Comptes Rendus Physique* **5** (2004) 955 [`hep-th/0410021`].

[101] M. B. Green, J. H. Schwarz and L. Brink, *N=4 Yang-Mills and N=8 Supergravity as Limits of String Theories*, *Nucl. Phys.* **B198** (1982) 474.

[102] Z. Bern, S. Davies, T. Dennen and Y.-t. Huang, *Absence of Three-Loop Four-Point Divergences in N=4 Supergravity*, *Phys.Rev.Lett.* **108** (2012) 201301 [`1202.3423`].

[103] S. Catani and M. H. Seymour, *The Dipole formalism for the calculation of QCD jet cross-sections at next-to-leading order*, *Phys. Lett.* **B378** (1996) 287 [`hep-ph/9602277`].

[104] S. Catani and M. H. Seymour, *A General algorithm for calculating jet cross-sections in NLO QCD*, *Nucl. Phys.* **B485** (1997) 291 [`hep-ph/9605323`].

[105] S. Catani, *The Singular behavior of QCD amplitudes at two loop order*, *Phys. Lett.* **B427** (1998) 161 [`hep-ph/9802439`].

[106] B. de Wit, *Supergravity*, in *Unity from duality: Gravity, gauge theory and strings. Proceedings, NATO Advanced Study Institute, Euro Summer School, 76th session, Les Houches, France, July 30-August 31, 2001*, pp. 1–135, 2002, `hep-th/0212245`.

[107] C. Cheung and D. O'Connell, *Amplitudes and Spinor-Helicity in Six Dimensions*, *JHEP* **0907** (2009) 075 [`0902.0981`].

[108] R. Boels, *Covariant representation theory of the Poincare algebra and some of its extensions*, *JHEP* **01** (2010) 010 [`0908.0738`].

[109] T. Dennen, Y.-t. Huang and W. Siegel, *Supertwistor space for 6D maximal super Yang-Mills*, *JHEP* **04** (2010) 127 [`0910.2688`].

[110] Z. Bern, J. J. Carrasco, T. Dennen, Y.-t. Huang and H. Ita, *Generalized Unitarity and Six-Dimensional Helicity*, *Phys.Rev.* **D83** (2011) 085022 [`1010.0494`].

[111] Y.-t. Huang, *Non-Chiral S-Matrix of N=4 Super Yang-Mills*, `1104.2021`.

[112] H. Elvang, Y.-t. Huang and C. Peng, *On-shell superamplitudes in N < 4 SYM*, *JHEP* **1109** (2011) 031 [`1102.4843`].

[113] J. C. Collins, *Renormalization*, vol. 26 of *Cambridge Monographs on Mathematical Physics*. Cambridge University Press, Cambridge, 1986, 10.1017/CBO9780511622656.

[114] G. 't Hooft and M. J. G. Veltman, *Regularization and Renormalization of Gauge Fields*, *Nucl. Phys.* **B44** (1972) 189.

[115] C. Gnendiger et al., *To d, or not to d: recent developments and comparisons of regularization schemes*, *Eur. Phys. J.* **C77** (2017) 471 [`1705.01827`].

[116] Z. Bern, S. Davies, T. Dennen, Y.-t. Huang and J. Nohle, *Color-Kinematics Duality for Pure Yang-Mills and Gravity at One and Two Loops*, *Phys. Rev.* **D92** (2015) 045041 [`1303.6605`].

[117] J. Nohle, *Color-Kinematics Duality in One-Loop Four-Gluon Amplitudes with Matter*, *Phys.Rev.* **D90** (2014) 025020 [`1309.7416`].

[118] A. Ochirov and P. Tourkine, *BCJ duality and double copy in the closed string sector*, *JHEP* **05** (2014) 136 [`1312.1326`].

[119] S. Badger, G. Mogull and T. Peraro, *Local integrands for two-loop QCD amplitudes*, in *13th DESY Workshop on Elementary Particle Physics: Loops and Legs in Quantum Field Theory (LL2016) Leipzig, Germany, April 24-29, 2016*, 2016, `1607.00311`, http://inspirehep.net/record/1473353/files/arXiv:1607.00311.pdf.

[120] S. Caron-Huot and K. J. Larsen, *Uniqueness of two-loop master contours*, *JHEP* **10** (2012) 026 [`1205.0801`].

[121] Z. Bern, J. Carrasco, H. Ita, H. Johansson and R. Roiban, *On the Structure of*

Supersymmetric Sums in Multi-Loop Unitarity Cuts, *Phys.Rev.* **D80** (2009) 065029 [0903.5348].

[122] G. Kälin, *Scattering Amplitudes in Supersymmetric Quantum Chromodynamics and Gravity*, Ph.D. thesis, Acta Universitatis Upsaliensis, 2019. http://urn.kb.se/resolve?urn=urn:nbn:se:uu:diva-381772.

[123] Z. Bern, J. J. Carrasco, W.-M. Chen, H. Johansson and R. Roiban, *Gravity Amplitudes as Generalized Double Copies of Gauge-Theory Amplitudes*, *Phys. Rev. Lett.* **118** (2017) 181602 [1701.02519].

[124] Z. Bern, J. J. M. Carrasco, W.-M. Chen, H. Johansson, R. Roiban and M. Zeng, *Five-loop four-point integrand of N = 8 supergravity as a generalized double copy*, *Phys. Rev.* **D96** (2017) 126012 [1708.06807].

[125] Z. Bern, J. J. Carrasco, W.-M. Chen, A. Edison, H. Johansson, J. Parra-Martinez et al., *Ultraviolet Properties of $\mathcal{N} = 8$ Supergravity at Five Loops*, *Phys. Rev.* **D98** (2018) 086021 [1804.09311].

[126] G. Mogull and D. O'Connell, *Overcoming Obstacles to Colour-Kinematics Duality at Two Loops*, *JHEP* **12** (2015) 135 [1511.06652].

[127] N. Arkani-Hamed, J. L. Bourjaily, F. Cachazo, A. Postnikov and J. Trnka, *On-Shell Structures of MHV Amplitudes Beyond the Planar Limit*, *JHEP* **1506** (2015) 179 [1412.8475].

[128] Z. Bern, E. Herrmann, S. Litsey, J. Stankowicz and J. Trnka, *Logarithmic Singularities and Maximally Supersymmetric Amplitudes*, *JHEP* **06** (2015) 202 [1412.8584].

[129] J. Drummond, J. Henn, G. Korchemsky and E. Sokatchev, *Generalized unitarity for N=4 super-amplitudes*, *Nucl.Phys.* **B869** (2013) 452 [0808.0491].